nature plants

Article

https://doi.org/10.1038/s41477-023-01583-x

Subtilase-mediated biogenesis of the expanded family of SERINE RICH ENDOGENOUS PEPTIDES

Received: 10 December 2022

Accepted: 3 November 2023

Published online: 4 December 2023

Check for updates

Huanjie Yang[1,8], Xeniya Kim[1], Jan Skłenar[2], Sébastien Aubourg[3], Gloria Sancho-Andrés[4], Elia Stahl[5], Marie-Charlotte Guillou[3], Nora Gigli-Bisceglia[6,9], Loup Tran Van Canh[3], Kyle W. Bender[1], Annick Stintzi[7], Philippe Reymond[5], Clara Sánchez-Rodríguez[4], Christa Testerink[6], Jean-Pierre Renou[3], Frank L. H. Menke[2], Andreas Schaller[7], Jack Rhodes[2] ✉ & Cyril Zipfel[1,2] ✉

Plant signalling peptides are typically released from larger precursors by proteolytic cleavage to regulate plant growth, development and stress responses. Recent studies reported the characterization of a divergent family of Brassicaceae-specific peptides, SERINE RICH ENDOGENOUS PEPTIDES (SCOOPs), and their perception by the leucine-rich repeat receptor kinase MALE DISCOVERER 1-INTERACTING RECEPTOR-LIKE KINASE 2 (MIK2). Here, we reveal that the SCOOP family is highly expanded, containing at least 50 members in the Columbia-0 reference *Arabidopsis thaliana* genome. Notably, perception of these peptides is strictly MIK2-dependent. How bioactive SCOOP peptides are produced, and to what extent their perception is responsible for the multiple physiological roles associated with MIK2 are currently unclear. Using N-terminomics, we validate the N-terminal cleavage site of representative PROSCOOPs. The cleavage sites are determined by conserved motifs upstream of the minimal SCOOP bioactive epitope. We identified subtilases necessary and sufficient to process PROSCOOP peptides at conserved cleavage motifs. Mutation of these subtilases, or their recognition motifs, suppressed PROSCOOP cleavage and associated overexpression phenotypes. Furthermore, we show that higher-order mutants of these subtilases show phenotypes reminiscent of *mik2* null mutant plants, consistent with impaired PROSCOOP biogenesis, and demonstrating biological relevance of SCOOP perception by MIK2. Together, this work provides insights into the molecular mechanisms underlying the functions of the recently identified SCOOP peptides and their receptor MIK2.

A growing number of plant signalling peptides are being identified and found to play major roles during growth, development and stress responses[1–3]. Such peptides are generally derived from protein precursors; however, relatively few biogenesis mechanisms have been described[2,4–9]. Some plant signalling peptides act as phytocytokines, which are secreted cell-to-cell mobile signals that regulate plant immune responses, analogous to cytokines in metazoans[10–12]. SERINE RICH ENDOGENOUS PEPTIDES (SCOOPs) have recently been reported

A full list of affiliations appears at the end of the paper. ✉e-mail: jack.rhodes@tsl.ac.uk; cyril.zipfel@botinst.uzh.ch

as a family of phytocytokines transcriptionally induced during stress, especially during biotic interactions[13–15]. SCOOPs are serine rich, derived from the C terminus of divergent secreted PROSCOOPs and are characterized by the presence of a 13–15 amino acid conserved epitope that includes an 'SxS' motif essential for bioactivity[13–15]. PROSOCOOPs undergo maturation steps to produce bioactive SCOOPs[14,16]. Cleavage of PROSCOOP12 was reported to be after R43 (ref. 14). For PROSCOOP10, two distinct cleaved peptides (SCOOP10#1 and SCOOP10#2) with hydroxylated prolines were identified from leaf apoplastic fluids[16]. The exact length of cleaved SCOOPs produced in planta and the proteases involved are, however, unknown. Also, given that synthetic unmodified 13- or 15-amino acid SCOOP peptides are bioactive[13–15,17], the exact role of potential posttranslational modifications of SCOOPs in planta is still unclear. Although initially reported as a 14-member family in the genome of the Columbia (Col-0) ecotype of *Arabidopsis thaliana* (later referred to as *Arabidopsis*)[13], the SCOOP family has recently been shown to contain up to 28 members[14,17]. Active SCOOP peptides induce cellular outputs typical of pattern-triggered immunity such as the production of apoplastic reactive oxygen species (ROS), rapid increase in cytosolic Ca^{2+} concentration and immune gene expression[13–15,17]. Among SCOOPs, SCOOP12—the founding member of the family—has been studied in more depth and was shown genetically to regulate immunity to diverse pathogens and pests, as well as root growth and ROS homeostasis[13,18,19]. SCOOPs are perceived by the *Arabidopsis* leucine-rich repeat receptor kinase MALE DISCOVERER 1-INTERACTING RECEPTOR LIKE KINASE 2 (MIK2) and recruit the BRASSINOSTEROID INSENSITIVE 1-ASSOCIATED KINASE 1(BAK1) as coreceptor[14,15]. Interestingly, MIK2 is involved in multiple diverse aspects of plant biology, such as responses to the cellulose biosynthesis inhibitor isoxaben (ISX), root growth angle, salt stress tolerance, resistance to the root vascular fungal pathogen *Fusarium oxysporum* 5176 and the generalist herbivore *Spodoptera littoralis*, as well as responsiveness to immune elicitors[14,15,19–23]. Although MIK2 is the sole SCOOP receptor, to which extent the multiple functions of MIK2 are all depending on SCOOP perception is still unknown.

Like most signalling peptides, SCOOPs undergo proteolytic processing to generate an active mature peptide in planta; however, little is known mechanistically about this process[14,15]. Many signalling peptides are cleaved by the subtilisin-like serine proteinases (subtilases, SBTs), which have been shown to cleave signalling peptides in a sequence- and modification-specific manner to generate bioactive peptides[24,25].

Here, we report a comprehensive annotation of *PROSCOOP* genes in the *Arabidopsis* Col-0 genome revealing the existence of 50 putative SCOOP peptides, at least 37 of which exhibited MIK2-dependent biological activity, making the SCOOPs one of the largest families of signalling peptides identified in flowering plants. Based upon co-expression during biotic stress, we identify several proteases from subtilase subgroup 3 transcriptionally responsive to the same environmental stimuli as *MIK2*, including biotic elicitor treatment, which promote PROSCOOP cleavage and are required for PROSCOOP activity in planta. Finally, we show that higher-order subtilase mutants phenocopy *mik2* mutants suggesting impaired SCOOP signalling.

Results

Identification of *PROSCOOP* genes within Col-0 genome

Originally, 14 *PROSCOOP* genes were identified in the *Arabidopsis* Col-0 genome[13]. Recently, tolerating more divergence in the core motif, this number was expanded to 23, and then 28 genes[14,17], highlighting the need for a revised bioinformatic analysis of the PROSCOOP family. We comprehensively re-evaluated the PROSCOOP repertoire through iterative searches using BLASTP/TBLASTN and the Motif Alignment & Search Tool (part of the MEME suite)[26]. Using this approach, we identified 22 additional putative PROSCOOPs, which we named PROSCOOP29 to PROSCOOP50 according to their location in the genome (Extended Data Fig. 1 and Supplementary Tables 1 and 2). Despite having low amino acid sequence similarity, all predicted SCOOP peptides have the conserved 'SxS' motif (Extended Data Fig. 1) previously shown to be required for activity[13–15]. Interestingly, all of the 30 *PROSCOOP* transcripts detected in our recent RNA sequencing dataset[27] are upregulated upon elicitor treatment (Extended Data Fig. 2), consistent with their possible function as phytocytokines. Interestingly, some SCOOPs correspond to previously annotated peptides, such as SECRETED TRANSMEMBRANE PEPTIDES[14,15,28], ENHANCER OF VASCULAR WILT RESISTANCE 1 (refs. 17,29) and ARACINs[30] (Supplementary Table 2). Notably, some of these peptides were previously shown to have direct antimicrobial activity[28,30], suggesting that PROSCOOPs are analogous to metazoan host-defence peptides encoding dual activities as both immunomodulatory phytocytokines and antimicrobial peptides[31].

Bioactive SCOOPs are MIK2- and BAK1-dependent

To test whether the newly identified SCOOPs are bioactive, we synthesized all of the corresponding 13-amino acid peptides, and found that many of them induced ROS production and triggered cytosolic Ca^{2+} fluxes when applied exogenously to Col-0 plants (Fig. 1a,b). Importantly, these responses were abolished in *mik2-1* (Extended Data Fig. 3a,b). Notably, whereas a 13-amino acid peptide is defined as the minimal active epitope for SCOOP12 (refs. 13–15), the length of a minimal active epitope appears to vary within the family. For example, the 13-amino acid peptide derived from SCOOP8 is inactive, but a 15-amino acid peptide that includes two additional N-terminal amino acids is active (Extended Data Fig. 3c)[14]. Thus, for a selection of inactive 13-amino acid peptides, we synthesized the corresponding 15-amino acid peptides and tested their activity. Several such 15-amino acid peptides (for example, SCOOP14 and SCOOP40) could induce MIK2-dependent ROS production (Fig. 1c and Extended Data Fig. 3d). In our assays, a few SCOOPs (for example, SCOOP29, SCOOP35, SCOOP38, SCOOP42 and SCOOP48) remained inactive (either as 13- or 15-amino acid peptides) (Fig. 1 and Extended Data Fig. 4), warranting further investigation of these SCOOPs in the future.

Overall, our data demonstrate that the *Arabidopsis* SCOOP family contains at least 50 members, and that all tested active synthetic SCOOP peptides induce MIK2-dependent responses (Extended Data Fig. 4). In addition, all tested active SCOOPs induce BAK1-dependent ROS production (Extended Data Fig. 3e), indicating that SCOOPs induce MIK2–BAK1 complex formation.

These findings thus define SCOOPs as one of the largest families of plant signalling peptides currently known. Strikingly, whereas other large signalling peptide families, such as CLAVATA3/ENDOSPERM SURROUNDING REGION-RELATED peptides, are perceived by several phylogenetically related receptors[32], the perception of all active SCOOP peptides is mediated by a single receptor, MIK2, making this ligand–receptor pair unique within the plant kingdom. Future structural work is required to define the molecular basis of SCOOP binding by MIK2. Some of the synthesized SCOOPs are inactive (Extended Data Fig. 4), possibly because the length and/or posttranslational modifications of peptides are important for activity. Some SCOOPs might also be perceived by another receptor that was lost in Col-0. It is also possible that the SCOOPs could possess other bioactivities, for example direct antimicrobial activity, or they may have become pseudogenized. These are interesting questions to pursue in future work.

PROSCOOP12 is cleaved by SBT3.5

Although PROSCOOPs have been shown to undergo proteolytic cleavage[14], the mechanisms by which bioactive SCOOPs are released from PROSCOOPs is still unknown. From the PROSCOOP sequence alignment (Extended Data Fig. 1), we noticed that most PROSCOOPs contain a 'RxLx/RxxL' motif that is recognized and cleaved by some SBTs including SBT6.1 and SBT3.5 (refs. 33–37). Using Genevestigator[38], we observed that among 56 *SBT* genes in *Arabidopsis*[37], *SBT3.3*, *SBT3.4* and *SBT3.5* are transcriptionally upregulated with *MIK2* under different conditions (Extended Data Fig. 5a). These phylogenetically

https://doi.org/10.1038/s41477-023-01583-x

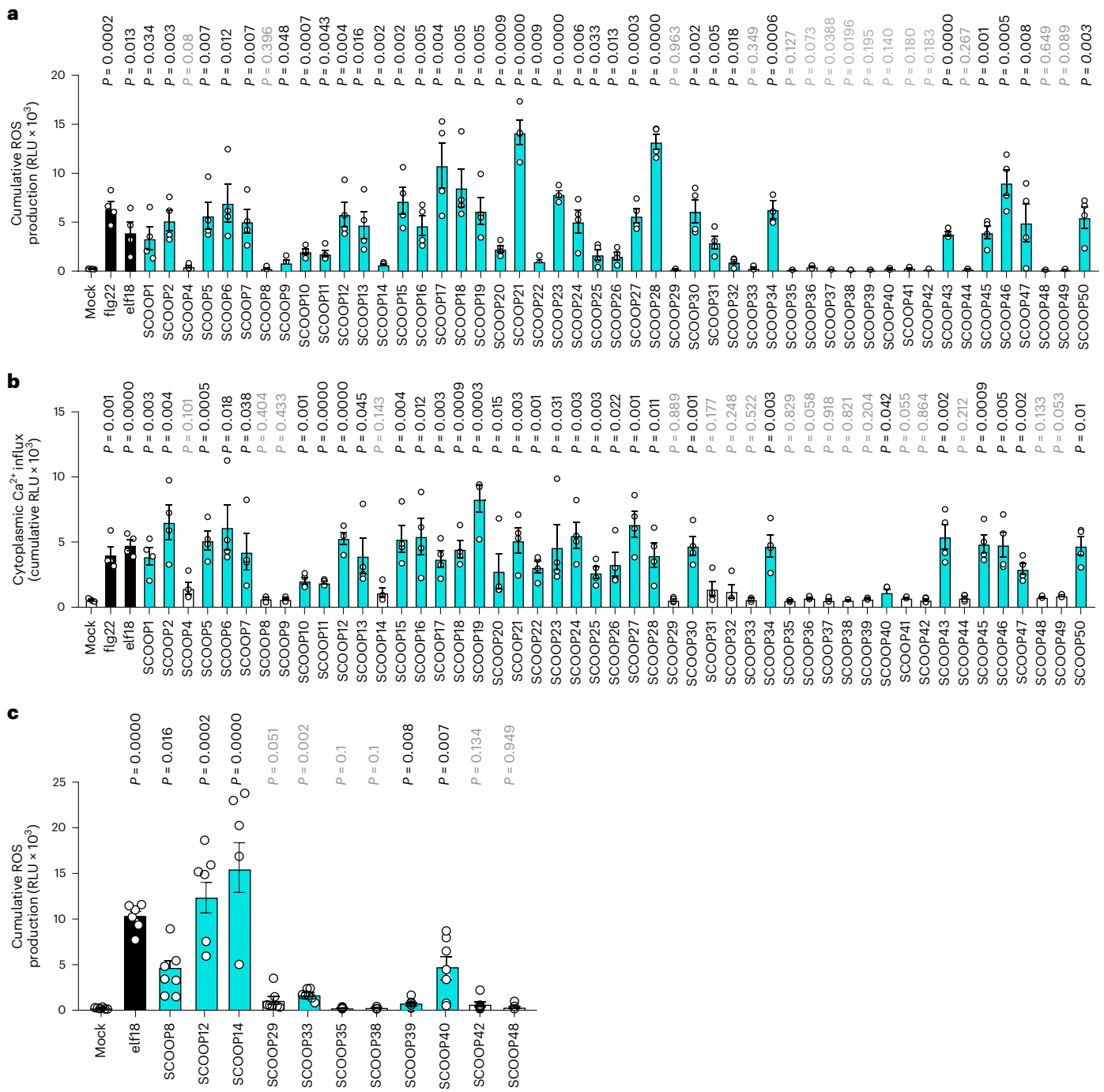

Fig. 1 | Divergent SCOOPs induce ROS production and Ca^{2+} influx in Col-0. **a**, Integrated ROS production over 40 min in leaf discs collected from 4-week-old plants induced in the absence (mock) or presence of 1 µM 13-amino acid SCOOP peptides ($n = 4$). flg22 and elf18 (100 nM) were used as controls. **b**, Cytoplasmic Ca^{2+} influx in Col-0^{AEQ} seedlings induced in the absence (mock) or presence of 1 µM 13-amino acid SCOOP peptides ($n = 4$) as measured by total relative light unit (RLU) emission over 25 min. flg22 and elf18 (100 nM) were used as controls. **c**, Integrated ROS production over 40 min in leaf discs collected from 4-week-old plants induced in the absence (mock) or presence of 1 µM 15-amino acid SCOOPs ($n = 5$) using 100 nM elf18 as control. RLU,. Data represent the mean ± s.d. *P* values indicate significance relative to the mock in a two-tailed *t*-test, grey text indicates $P > 0.05$. All experiments were repeated and analysed three times with similar results.

related *SBT* genes were also among the most upregulated in response to elicitor treatments (Extended Data Fig. 5b,c)[27,39]. Notably, SBT3.3 and SBT3.5 have previously been shown to regulate plant immunity and root growth, respectively[37,40], similar to PROSCOOP12 (refs. 13,19). Also, SBT3.5 has a preference for the RKLL motif[37], which is similar to a motif found in many PROSCOOP sequences (Extended Data Fig. 1). To test whether related SBT3 proteases can cleave PROSCOOPs at such a motif, we focused on PROSCOOP12, the best-characterized PROSCOOP with strong activity[13–15,18,19]. We chose to test cleavage using *Agrobacterium*-mediated transient expression in *Nicotiana benthamiana*, a plant species that does not contain *SBT3* or *PROSCOOP* genes in its genome[41], thus enabling gain-of-function experiments. As a probe for proteolytic cleavage, we inserted a 6xHA tag between the predicted native signal peptide and PROSCOOP12 coding sequence

https://doi.org/10.1038/s41477-023-01583-x

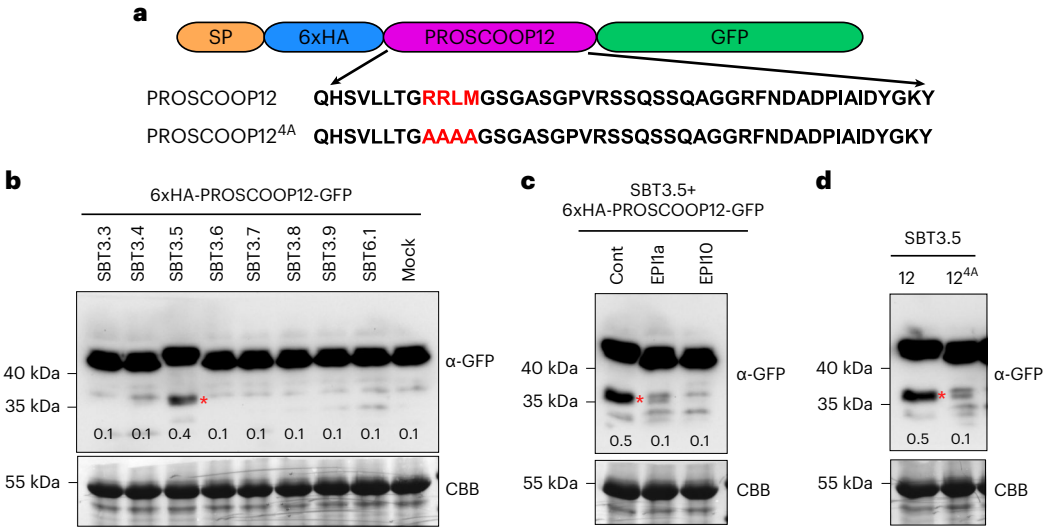

Fig. 2 | PROSCOOP12 is cleaved by SBT3.5. a, Schematic representation of PROSCOOP12 with native signal peptide (SP), N-terminal 6xHA tag and C-terminal GFP tag. The cleavage motif RRLM and mutated residues of RRLM/AAAA are shown as red characters. **b**–**d**, Western blot using GFP antibody recognizing the 6xHA-PROSCOOP12-GFP and truncated SCOOP12-GFP (indicated by the red asterisk) in *N. benthamiana* leaves after 100 nM flg22 treatment for 2 h. The membrane was stained with Coomassie brilliant blue (CBB), as a loading control. Numbers on the blots correspond to the ratios of protein accumulation levels between truncated proteins bands (indicated by the red asterisk) and full-length protein bands (above the truncated protein bands). Transient co-expression of: 6xHA-PROSCOOP12-GFP with SBT3.3, SBT3.4, SBT3.5, SBT3.6, SBT3.7, SBT3.8, SBT3.9, SBT6.1 or without SBT (mock) (**b**); 6xHA-PROSCOOP12-GFP, SBT3.5 with SBT inhibitors EPI1a/EPI10 or without SBT inhibitor (mock (Cont)) (**c**); and SBT3.5 with 6xHA-PROSCOOP12-GFP (labelled as 12) or 6xHA-PROSCOOP12^{4A}-GFP (labelled as 12^{4A}) (**d**). All experiments were repeated and analysed three times with similar results.

fused to an in-frame C-terminal green fluorescent protein (GFP) tag (SP-6xHA-PROSCOOP12-GFP) (Fig. 2a). We then co-expressed this construct with untagged SBT3s (because the presence of a tag could affect SBT protease activity[42–44]). Notably, expression of SBT3.5 resulted in the increased accumulation of a lower molecular weight protein band under flg22 treatment (Fig. 2b and Extended Data Fig. 6; indicated by a red asterisk) at a size corresponding to SCOOP12-GFP. However, it is not clear whether SBT3.3 and SBT 3.4 could cleave PROSCOOP12 in our assays. It could be that SBT3.3 and SBT3.4 cleavage activity is too weak to be detected in this assay. The basal level of the cleaved SCOOP12-GFP products could be caused by endogenous SBTs or other proteases in *N. benthamiana*.

To test the dependency upon SBT3.5's enzymatic activity, we made use of the specific subtilase inhibitors, EXTRACELLULAR PROTEINASE INHIBITOR 1a and 10 (EPI1a and EPI10), normally produced by the plant pathogen *Phytophthora infestans* as virulence effectors, which have been used previously to assess SBT's functions[4,6,45–48]. As expected, SBT3.5-induced accumulation of the PROSCOOP12 cleavage product was reduced when EPI1a and EPI10 were co-expressed (Fig. 2c). We next sought to establish the importance of the putative SBT cleavage motif present in PROSCOOP sequences. Mutation of RRLM into AAAA strongly reduced cleavage of PROSCOOP12 by SBT3.5 (Fig. 2d). A previous study showed that PROSCOOP12 is processed at RRLM motif but cleaved downstream of RR[14]. Using mass spectrometry (MS) coupled with N-terminal labelling (Extended Data Fig. 7), we identified the GSGAGPVR peptide as the N terminus of the SCOOP12-GFP cleavage product (Extended Data Fig. 8a), suggesting the cleavage site is after the RRLM motif in planta. Together, these data indicate SBT3.5 can cleave PROSCOOP12 to release active SCOOP12.

PROSCOOP20 is cleaved by SBT3.6, SBT3.8 and SBT3.9

In addition to PROSCOOPs containing a 'RxLx/RxxL' motif, we noticed a subgroup of PROSCOOPs that lack the 'RxLx/RxxL' motif but instead contain a 'VWD' motif (Extended Data Fig. 1), a previously reported cleavage motif for the aspartate-dependent subtilase SBT3.8 (refs. 5,49). *SBT3.6*, *SBT3.7*, *SBT3.9* and *SBT3.10* are *SBT3.8* homologues (Extended Data Fig. 5c[39]) and *SBT3.7*, *SBT3.9* and *SBT3.10* are highly upregulated by elicitors treatment (Extended Data Fig. 5b). We hypothesized that PROSCOOPs containing the VWD motif could be cleaved by SBT3.8 or its paralogues. To test this, we selected *PROSCOOP20*, which we recently identified as a 'core immunity response' gene[27]. Using a similar approach, we co-expressed SP-6xHA-PROSCOOP20-GFP (Fig. 3a) with different SBT3s. This resulted in the identification of several protein products as identified by SDS–polyacrylamide gel electrophoresis (SDS–PAGE) α-GFP western blot (Fig. 3b). We found that expression of SBT3.6, SBT3.8 and SBT3.9 led to an increased accumulation of a lower molecular weight protein band, indicative of SCOOP20-GFP (Fig. 3b).

Notably, expression of SBT3.3, 3.4, 3.5 or 3.7 had no apparent effect on PROSCOOP20 cleavage (Fig. 3b), whereas expression of SBT3.3, 3.4, 3.6, 3.7, 3.8 or 3.9 did not affect PROSCOOP12 cleavage, underlining the specificity of distinct PROSCOOPs cleavage by the different SBTs identified (Fig. 2b). The well-characterized subtilase SBT6.1/S1P did not seem to affect either PROSCOOP12 or PROSCOOP20 cleavage (Figs. 2b and 3b). The ability of the tested SBTs to induce PROSCOOP cleavage thus seems to correlate with the presence of distinct potential cleavage motifs (RRLM for PROSCOOP12, VWD for PROSCOOP20).

The increased accumulation of the cleaved band was reduced by co-expression with the inhibitors EPI1a and EPI10 (Fig. 3c). Similarly, mutation of the predicted 'VWD' motif into 'AAA' (PROSCOOP20^{3A}) reduced PROSCOOP20 cleavage by SBT3.8 (Fig. 3d). These data suggest PROSCOOP20 cleavage is dependent on SBT3.8 activity.

Using N-terminal labelling-coupled MS (Extended Data Fig. 7), DLKIGASGSNSG peptide was detected (Extended Data Fig. 8b), whereas TLLRDLKIGASGSNSG (Extended Data Fig. 8c) was only detected once from three replicates, suggesting there could be another cleavage site after the VWD motif to produce mature SCOOP20.

We next sought to genetically characterize the role of SBT3.8 in *Arabidopsis*. We were concerned about genetic redundancy because several SBT3.8 paralogues were able to promote PROSCOOP20 cleavage in planta, so we decided to generate a higher-order *sbt3.6/7/8/9/10* mutant using CRISPR–Cas9[41] (Extended Data Fig. 9). This was facilitated by the tandem genomic arrangement of related SBT3s (Extended Data

https://doi.org/10.1038/s41477-023-01583-x

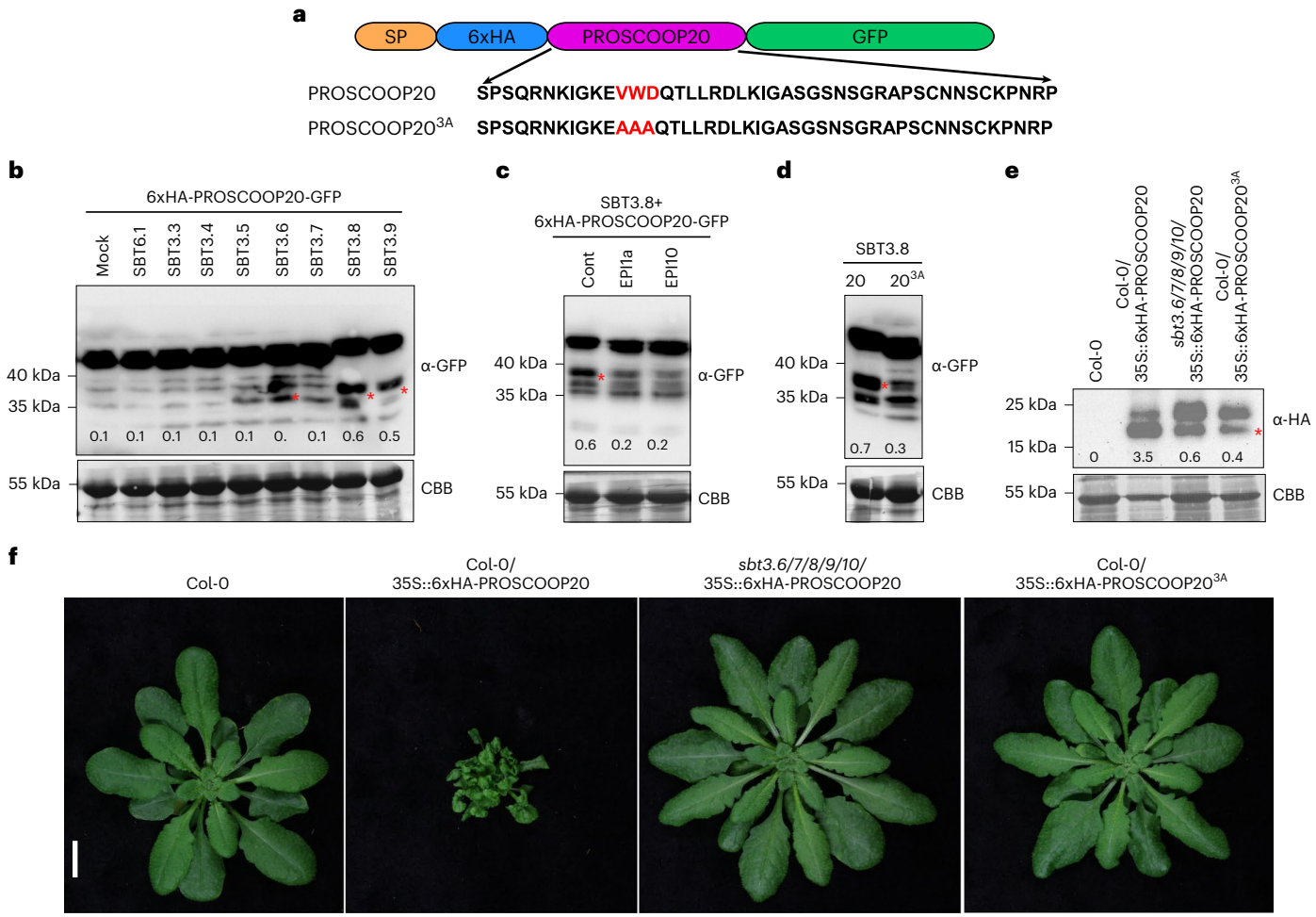

Fig. 3 | PROSCOOP20 is cleaved by SBT3.6, SBT3.8 and SBT3.9. a, Schematic representation of PROSCOOP20 with native signal peptide (SP), N-terminal 6xHA tag and C-terminal GFP tag. The cleavage motif VWD and mutated residues of VWD/AAA are shown as red characters. **b**–**d**, Western blot using GFP antibody recognizing the 6xHA-PROSCOOP20-GFP and truncated SCOOP20-GFP (indicated by the red asterisk) in *N. benthamiana* leaves after 100 nM flg22 treatment for 2 h. The membrane was stained with Coomassie brilliant blue (CBB) as a loading control. Numbers on the blots correspond to the ratios of protein accumulation levels between truncated proteins bands (indicated by the red asterisk) and full-length protein bands (above the truncated proteins bands). Transient co-expression of: 6xHA-PROSCOOP20-GFP with or without SBT3.3, SBT3.4, SBT3.5, SBT3.6, SBT3.7, SBT3.8, SBT3.9, SBT6.1 (mock) (**b**); 6xHA-PROSCOOP-GFP, SBT3.8 with SBT inhibitors EPI1a/EPI10 or without (mock) (**c**); and SBT3.8 with 6xHA-PROSCOOP20-GFP (labelled as 20) or 6xHA-PROSCOOP20^{3A}-GFP (labelled as 20^{3A}) (**d**). All experiments were repeated and analysed three times with similar results. **e**, Western blot using HA antibody recognizing the 6xHA-PROSCOOP20 in stable transgenic *Arabidopsis* seedings expressing 35S::6xHA-PROSCOOP20 (labelled as 20) or 35S::6xHA-PROSCOOP20^{3A} (labelled as 20^{3A}) in Col-0 or *sbt3.6/7/8/9/10*. The membrane was stained with CBB as a loading control. Numbers on the blots are the ratios of protein accumulation levels between truncated protein bands (indicated by the red asterisk) and full-length protein bands (above the truncated protein bands). The experiment was repeated independently three times with similar results. **f**, Phenotype of stable transgenic *Arabidopsis* seedlings expressing 35S::6xHA-PROSCOOP20 or 35S::6xHA-PROSCOOP20^{3A} in Col-0 or *sbt3.6/7/8/9/10*. Scale bar, 1 cm.

Fig. 5c). Notably, whereas overexpression of PROSCOOP20 in Col-0 caused a dwarf rosette phenotype, loss of SBT3.6/7/8/9/10 or the processing motif VWD (which was mutated into AAA) suppressed this phenotype (Fig. 3f,e). Together, these data indicate that SBT3.8 and potentially related SBTs mediate the cleavage of PROSCOOP20 around the VWD motif, which is required for SCOOP20-induced signalling.

Loss of *SBT3*s partially phenocopies the loss of *MIK2*

Our study revealed that the SCOOP family is much larger than previously predicted, which renders the genetic characterization of these peptides challenging. Because we could demonstrate that different subgroup 3 SBTs are involved in SCOOP cleavage, we generated an octuple mutant for SBT3.3, 3.4, 3.5, 3.6, 3.7, 3.8, 3.9 and 3.10 (*sbt3*^{octuple}) by crossing independent *sbt3.3/4/5* and *sbt3.6/7/8/9/10* mutants generated using CRISPR–Cas9 (Extended Data Fig. 9). The *sbt* higher-order mutants did not show any macroscopic growth and developmental phenotype (Extended Data Fig. 10a); however, the dry weight of *mik2-1* and *sbt*^{octuple} is marginally increased compared with Col-0 (Extended Data Fig. 10b). We hypothesized that the *sbt3*^{octuple} mutant is impaired in PROSCOOP processing, and thus provides a genetic background to test for the requirement of SCOOP recognition in different MIK2-dependent processes.

Notably, similar to what was observed in *mik2-1* (ref. 15), flg22-induced ROS production was impaired in *sbt3*^{octuple} plants (Fig. 4a,b), but not in *sbt3.3/4/5* or *sbt3.6/7/8/9/10* (Extended Data Fig. 10c). MIK2 is also involved in the induction of stress responses upon ISX treatment[21,22]. Induction of the stress marker genes *FRK1* and *CYP81F3* upon ISX treatment was similarly impaired in both *mik2-1* and *sbt3*^{octuple} seedlings (Fig. 4c). Moreover, it was recently demonstrated that MIK2 is required for basal resistance against the generalist herbivore *S. littoralis*[19]. This resistance—as determined by measuring the larvae fresh weight—was also impaired in *sbt3*^{octuple}, albeit to an intermediate level compared with *mik2-1* plants (Fig. 4d).

https://doi.org/10.1038/s41477-023-01583-x

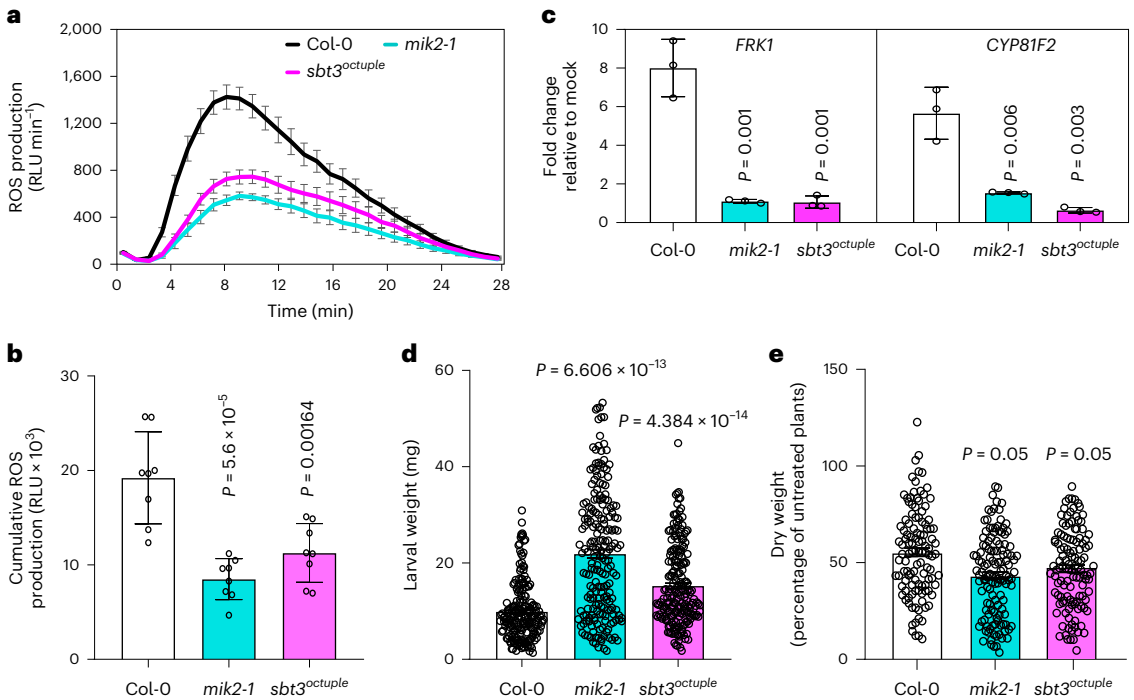

Fig. 4 | *sbt3*^{octuple} phenocopies *mik2*. **a**,**b**, ROS production in leaf discs collected from 4-week-old Arabidopsis plants induced by 100 nM flg22 ($n = 8$). Points represent mean ± s.d. (**a**). Integrated ROS production over 30 min (**b**). **c**, Immune marker genes expression in 13-day-old *Arabidopsis* seedlings determined by quantitative PCR with reverse transcription. Seedlings were treated with 0.6 µM ISX or mock. Expression of *FRK1* and *CYP81F2* was normalized relative to *Actin7* expression values. Depicted is the fold change in expression relative to mock treatment ($n = 3$). Data represent the mean ± s.d.; *P* values indicate significance relative to the mock in a two-tailed *t*-test. All experiments were repeated and analysed three times with similar results. **d**, Insect performance of *Spodoptera littoralis* on Col-0, *mik2-1* and *sbt3*^{octuple}. *S. littoralis* larvae were feeding on 5-week-old plants for 12 days. Data represent the mean ± s.d. of three independent experiments. *P* values indicate significance relative to Col-0 in a two-sided Mann–Whitney *U*-test. Number of individual larvae measured: Col-0, $n = 215$; *mik2-1*, $n = 204$; and *sbt3*^{octuple}, $n = 211$. **e**, Dry weight of NaCl-treated plants is expressed as percentage of the ratio to the dry weight of untreated plants. One week after germination, plants were transferred to pots with soil saturated with or without 75 mM of NaCl in demineralized water. After 3 weeks of treatment the rosettes were cut, and dry weight was determined. Data represent the mean ± s.d. of three independent experiments. *P* values indicate significance relative to Col-0 in a two-tailed *t*-test. Number of individual larvae measured: Col-0, $n = 114$; *mik2-1*, $n = 127$; *sbt3*^{octuple}, $n = 120$.

Discussion

These data suggest that the control of elicitor-induced ROS production, ISX-induced stress responses and basal resistance to *S. littoralis* all require SBT3 function, and thus by extension potential PROSCOOP processing and subsequent SCOOP perception by MIK2. However, it must be noted that these SBTs have other targets in planta, which may contribute to the phenotypes observed. For example, SBT3.8 also cleaves phytosulfokine and CLE-LIKE/GOVEN/ROOT GROWTH FACTOR peptides, which have reported roles in the regulation of immune signalling[4,49–52]. However, whereas MIK2 regulates root growth angle[21] and basal resistance to *F. oxysporum*[21,23], *sbt3*^{octuple} plants behaved as wild-type Col-0 plants in these assays (Extended Data Fig. 10d,e), which could be because of non-cleaved PROSCOOPs and the generation of bioactive SCOOPs from some PROSCOOP precursors via SBTs beyond those characterized in our study. Notably, the recent identification of native SCOOP10 peptides in leaf apoplastic fluids suggests that the cleavage of PROSCOOP10, which lacks 'RxLx/RxxL' and 'VWD' motifs, could be dependent upon Y[KR]PN motif reported as cleavage site of subtilases SBT4.12, SBT4.13 and SBT5.2 (refs. 6,16,24,25). Furthermore, it is possible that some of the phenotypes observed in the *mik2* mutant may be independent of its function as the SCOOP receptor. Moreover, the strong susceptibility of *mik2* mutant plants to *F. oxysporum*, which is not phenocopied by the loss of SBT3s, suggests that resistance against this fungus may be due to the direct perception of *F. oxysporum*-derived elicitors (potentially exhibiting SCOOP-like sequences) by MIK2 (refs. 14,15,23), which would not necessarily require proteolytic cleavage by a plant subtilase. The exact *F. oxysporum*-derived elicitor(s) recognized by MIK2 during infection however remain to be identified.

Collectively, our study provides additional information about the recently identified family of SCOOP peptides, their posttranslational processing and biological roles. Notably, because several SCOOPs have been previously proposed as antimicrobial peptides[28,30], it will be interesting to understand the evolutionary and biochemical basis of the dual activity of these SCOOPs. This work also provides a starting point to dissect the multiple functions of MIK2. Notably, it will be interesting in the future to identify which specific SCOOPs mediate these functions, as recently demonstrated for SCOOP12 in the context of herbivory and root growth[18,19].

Methods

Plant material and growth conditions

Arabidopsis thaliana Col-0 was used as a wild-type control. Plants for ROS burst assays were grown in individual pots at 21 °C with a 10 h photoperiod. Seeds grown on plates were surface-sterilized using chlorine gas for 5–6 h, and sown on Murashige and Skoog media supplemented with vitamins, 1% sucrose and 0.8% agar, and stratified at 4 °C for 2–3 days. *Nicotiana benthamiana* plants were grown on peat-based media at 24 °C, with a 16 h photoperiod.

Aequorin lines of *Arabidopsis* have been described previously[15,53], as have *mik2-1* and *sbt3.5-1* mutants[21,37].

Synthetic peptides

All synthetic peptides were ordered at >80% purity (physiological assays) or >95% purity (biochemical assays) (EZBiolab). Sequences of all peptides can be found in Supplementary Table 1. The gene

models from which the peptide sequences were extracted are listed in Supplementary Table 2.

Molecular cloning

These constructs below were generated by GreenGate cloning[54]. pGGZ-35S::SBT3.4 and pGGZ-35S::SBT3.9, pGGZ-35S::6xHA-PROSCOOP12-GFP, pGGZ-35S::6xHA-PROSCOOP12^{4A}(RRLM/AAAA)-GFP, pGGZ-35S::6xHA-PROSCOOP20-GFP, pGGZ-35S::6xHA-PROSCOOP20^{3A}(VWD/AAA)-GFP and pGGZ-35S::6xHA-PROSCOOP20, pGGZ-35S::6xHA-PROSCOOP20^{3A}(VWD/AAA).

The genomic DNA of *SBT3.4* and *SBT3.9* was amplified by PCR. The coding sequence of 6xHA-PROSCOOP12, 6xHA-PROSCOOP12^{4A} (RRLM/AAAA), 6xHA-PROSCOOP12 and 6xHA-PROSCOOP12^{3A}(VWD/AAAA) were synthesized. Clones were verified by Sanger sequencing.

pGreen0229-pPROSCOOP12::EPI1a/10 was generated by replacing the IDA promoter from the construct pGreen0229-pIDA::EPI1a/10[6]. Some 1,500 bp upstream of the start codon of the PROSCOOP12 gene were amplified by PCR using the primer (Supplementary Table 3). The PCR products and pGreen0229-pIDA::EPI1a/10 were digested with NotI and PstI. The PCR product was then cloned into the respective restriction sites of pGreen0229 upstream of the EPI1a or EPI10 constructs.

Expression constructs pART27-35S::SBT3.5 and pART7-35S::SBT3.8 have been described previously[5,37]. Expression constructs for SBT3.3 and SBT3.7 were generated accordingly. Briefly, the open reading frames of SBT3.3 and SBT3.7 were amplified by PCR and cloned into the multiple cloning site of pART7 (ref. 55), between the CaMV-35S promoter and terminator. The expression cassette was then transferred into the NotI site of the binary vector pART27 (ref. 55).

CRISPR–Cas9 mutagenesis

CRISPR–Cas9-induced mutagenesis was performed as described[56]. The *RPS5a* promoter drove Cas9 expression and FASTred selection was used for positive and negative selection. Primers used to generate the vectors can be found in Supplementary Table 3. Mutants were screened by PCR genotyping and confirmed by Sanger sequencing. Primers used for genotyping and sequencing can be found in Supplementary Table 3.

ROS measurement

Leaf discs were harvested from 4-week-old *Arabidopsis* plants using a 4-mm diameter biopsy punch (Integra Miltex) and placed into white 96-well plates (Greiner Bio-One, catalogue no. 655075) containing 100 µl of water. Leaf discs were rested overnight. Before ROS measurement, the water was removed and replaced with ROS assay solution (100 µM luminol; Merck, catalogue no. 123072), 20 µg ml^{-1} horseradish peroxidase (Merck, catalogue no. P6782)) with or without elicitors. Immediately after light emission was measured from the plate using a high-resolution photon counting system (Photek, catalogue no. HRPCS218) equipped with a 20 mm F1.8 EX DG aspherical RF wide lens (Sigma).

Cytoplasmic Ca^{2+} measurement

Seedlings were initially grown on ½ Murashige and Skoog plated for 3 days before transfer to 96-well plates (Greiner Bio-One, catalogue no. 655075) in 100 µl of liquid Murashige and Skoog for 5 days. The evening before Ca^{2+} measurements the liquid Murashige and Skoog was replaced with 100 µl of 20 µM coelenterazine (Carbosynth, catalogue no. EC14031) and the seedlings incubated in the dark overnight. The following morning the coelenterazine solution was replaced with 100 µl of water and rested for a minimum of 30 min in the dark. Readings were taken in a Varioskan mutiplate reader (Thermo Fisher Scientific) before and after adding 50 µl of 3× concentrated elicitor solution or mock.

CLANs clustering of PROSCOOP family

The 50 PROSCOOP sequences were analysed and clustered using CLANS software based on all-against-all BLASTP pairwise sequence similarities[57]. The *P* value cut-off was set to 1×10^{-2} for edge definition and the Convex method (s.d. cut-off 0.5, minimum of three sequences per cluster) has been applied for clustering. Details of the *PROSCOOP* sequences can be found in Supplementary Table 2. PROSCOOP34 (AT1G54945; Chr1_20486119.20486313) and PROSCOOP47 (AT5G36122; Chr5_14202369.14202451, 14202714.14202810) are newly annotated.

Transient expression in *Nicotiana benthamiana*

Agrobacterium tumefaciens strain GV3101 transformed with the appropriate construct was grown overnight in L-media and spun-down. The bacteria were resuspended in 10 mM $MgCl_2$ and adjusted to OD_{600} = 0.2 before infiltration into the youngest fully expanded leaves of 3-week-old plants. Two days later, leaf tissues were collected, treated in liquid Murashige and Skoog medium using 100 nM flg22 for 2 h and flash-frozen in liquid nitrogen.

Protein extraction and western blot

N. benthamiana leaf tissues were flash-frozen in liquid nitrogen. Plant tissue was ground in liquid nitrogen before boiling in 2× loading sample buffer (4% SDS, 20% glycerol, 10% 2-mercaptoethanol, 0.004% bromophenol blue, 0.125 M Tris–HCl; 10 µl per mg of tissue) for 10 min at 95 °C. The samples were then spun at 13,000*g* for 5 min before loading and running on SDS–PAGE gels of an appropriate concentration. Proteins were transferred onto a polyvinylidene difluoride membrane (Thermo Fisher Scientific) before incubation with appropriate antibodies (α-HA-HRP (Roche, catalogue no. 12013819001; 1:3,000) and α-GFP-HRP (Santa Cruz, catalogue no. sc-9996, 1:5,000). Western blots were imaged with a LAS 4000 ImageQuant system (GE Healthcare). Staining of the blotted membrane with Coomassie brilliant blue was used to confirm loading.

GFP-TRAP enrichment

After protein extraction from *N. benthamiana* leaf tissues, the 6xHA-PROSCOOP12/20-GFP and SCOOP12/20-GFP was enriched by GFP-Trap. Proteins were extracted using the extraction buffer (50 mM Tris pH 7.5, 150 mM NaCl, 2.5 mM EDTA, 10% glycerol, 1% IGEPAL, 5 mM dithiothreitol, 1% plant protease inhibitor (Sigma, catalogue no. P9599)) (v/v). Proteins were solubilized at 4 °C with gentle agitation for 30 min before filtering through miracloth. The filtrate was centrifuged at 15,000*g* for 20 min at 4 °C. An input sample was taken. To each 15 ml of protein extract was added 40 µl of GFP-Trap agarose beads (50% slurry, ChromoTek) washed in extraction buffer and the mixture was incubated with gentle agitation for 4 h at 4 °C. Beads were harvested by centrifugation at 1,500*g* for 2 min and washed three times in extraction buffer. Fifty microlitres of 1.5× elution buffer (NuPage) were added and incubated at 90 °C for 10 min. The samples were then spun at 13,000*g* for 5 min before loading and running on SDS–PAGE gels of an appropriate concentration. Samples were then cut from the SDS–PAGE gel for subsequent MS analysis.

N-terminal labelling and MS

Proteins separated by SDS–PAGE were excised, destained with 25% acetonitrile, reduced by 10 mM dithiothreitol 55 °C for 30 min and carbamidomethylated with 40 mM chloroacetamide. The gel was washed with copious exchanges of 50 mM TEAB and dehydrated with 100% acetonitrile. Protein free N termini were labelled with 100 µg TMT reagent (Thermo Fisher Scientific) dissolved in 20 µl of 100% acetonitrile and directly added to the gel followed by 80 µl of 50 mM TEAB (Thermo Fisher Scientific) buffer. The reaction was left at room temperature for 90 min and subsequently quenched with 5% hydroxylamine; after which, all proteoforms with accessible N termini should be N-terminally TMT-labelled.

The reagent leftovers were extracted by 50 mM ammonium bicarbonate buffer and the gel dehydrated with 100% acetonitrile. Proteins were in-gel digested by 100 ng of trypsin (Thermo Fisher Scientific),

peptides were extracted with 25% acetonitrile, freeze-dried and measured by Orbitrap Eclipse (Thermo Fisher Scientific) liquid chromatography–MS system with a data-dependent acquisition MS method.

The data were processed with a common proteomic pipeline consisting of MS Convert program to generate peak-lists followed by peptide sequence matching on Mascot (Matrix Science) server. The individual samples were compared and tandem mass spectra visualized in Scaffold (Proteome Software).

RNA extraction and quantitative PCR with reverse transcription

Two 5-day-old seedlings were transferred to transparent 24-well plates (Greiner Bio-One) containing 1 ml of liquid Murashige and Skoog media, sealed with porous tape and grown for a further 7 days. The liquid Murashige and Skoog media was removed and 1 ml of fresh liquid Murashige and Skoog medium containing 600 nM ISX (Sigma-Aldrich) or mock was added, and seedlings were harvested after 9 h treatment. All seedlings were ground in liquid nitrogen. Total RNA was extracted using plant total RNA mini kit (FavorPrep) according to the manufacturer's instructions and DNase treatment was performed using the RNeasy kit (Qiagen). RNA was quantified with a nanodrop spectrophotometer (Thermo Fisher Scientific). Quantitative PCR with reverse transcription was performed on complementary DNA synthesized using the RevertAid first-strand cDNA synthesis kit (Thermo Fisher Scientific) according to the manufacturer's instructions. cDNA was amplified by quantitative PCR using PowerUP SYBR Green Master mix (Thermo Fisher Scientific) running on an Applied Biosystems 7500 Fast Real-Time PCR System (Thermo Fisher Scientific).

Insect performance

Spodoptera littoralis (Egyptian cotton worm) eggs were obtained from Syngenta. For hatching, *S. littoralis* eggs were incubated for 48 h at 28 °C. For measurements of insect performance, 60–80 freshly hatched *S. littoralis* larvae were placed on eleven 5-week-old plants per genotype in transparent plexiglass boxes. *S. littoralis* larvae were allowed to feed on those plants for 12 days and individual larval weights were determined subsequently on a high precision balance (Mettler-Toledo, catalogue no. XP205DR).

Fusarium oxysporum 5176 infection assay

Plants were infected on plates as previously described[58,59]. Briefly, seeds were germinated on Whatman filter paper strips in ½ Murashige and Skoog + 0.9% agar. Eight-day-old seedling were transferred to a mock or infection plate. The infection plates were prepared by spreading 100 µl of 1×10^7 pSIX1:GFP spores per millilitre on the Murashige and Skoog + 0.9% bactoagar surface. Vascular penetration sites were recorded from 3 to 7 days post transfer to spore-containing plates, determined when strong and linear signals were visible under a Leica M205 FCA fluorescent stereomicroscope equipped with a long pass GFP filter (ET GFP LP; excitation nm: ET480/40x; emission nm: ET510 LP).

Root skewing assay

Seeds were sown directly on ½ Murashige and Skoog agar square plates and stratified for 2 days at 4 °C. Plates were transferred to 22 °C under a 16 h photoperiod, in an upright position for 9 days. The root angle was measured by the ImageJ software, as performed previously[21].

Salt tolerance assays

Salt tolerance assays were performed as previously[21]. Plants were grown in pots under an 11 h photoperiod, at 22 °C and 70% humidity. One week after germination, plants were transferred to pots which were saturated with 4 litres of either 0 or 75 mM of NaCl solution. During the experiment, all plants were watered with demineralized water from below. After 3 weeks of treatment, plants were cut-off and dried in an oven at 70 °C for 1 week to determine dry weight. Plants were randomized over trays using a randomized block design. Randomization was similar for each treatment. The experiment was repeated three times with similar results.

Statistical analysis

Statistical analysis was performed in GraphPad Prism v.10.0. (http://www.graphpad.com) unless stated otherwise. Dot plots were used to show individual data points wherever possible. *P* values <0.05 were considered non-significant. Sample sizes, statistical tests used, and *P* values are stated in the figure legends.

Reporting summary

Further information on research design is available in the Nature Portfolio Reporting Summary linked to this article.

Data availability

The authors declare that the data supporting the findings of this study are available within the manuscript and its supplementary files. Source data are provided with this paper.

References

1. Matsubayashi, Y. Posttranslationally modified small-peptide signals in plants. *Annu. Rev. Plant Biol.* **65**, 385–413 (2014).
2. Olsson, V. et al. Look closely, the beautiful may be small: precursor-derived peptides in plants. *Annu. Rev. Plant Biol.* **70**, 153–186 (2019).
3. Tavormina, P., De Coninck, B., Nikonorova, N., De Smet, I. & Cammue, B. P. The plant peptidome: an expanding repertoire of structural features and biological functions. *Plant Cell* **27**, 2095–2118 (2015).
4. Stührwohldt, N., Ehinger, A., Thellmann, K. & Schaller, A. Processing and formation of bioactive CLE40 peptide are controlled by posttranslational proline hydroxylation. *Plant Physiol.* **184**, 1573–1584 (2020).
5. Stührwohldt, N. et al. The biogenesis of CLEL peptides involves several processing events in consecutive compartments of the secretory pathway. *eLife* **9**, e55580 (2020).
6. Schardon, K. et al. Precursor processing for plant peptide hormone maturation by subtilisin-like serine proteinases. *Science* **354**, 1594–1597 (2016).
7. Reichardt, S., Piepho, H. P., Stintzi, A. & Schaller, A. Peptide signaling for drought-induced tomato flower drop. *Science* **367**, 1482–1485 (2020).
8. Doll, N. M. et al. A two-way molecular dialogue between embryo and endosperm is required for seed development. *Science* **367**, 431–435 (2020).
9. Stührwohldt, N. & Schaller, A. Regulation of plant peptide hormones and growth factors by post-translational modification. *Plant Biol.* **21**, 49–63 (2019).
10. Rzemieniewski, J. & Stegmann, M. Regulation of pattern-triggered immunity and growth by phytocytokines. *Curr. Opin. Plant Biol.* **68**, 102230 (2022).
11. Hou, S., Liu, D. & He, P. Phytocytokines function as immunological modulators of plant immunity. *Stress Biol.* **1**, 8 (2021).
12. Gust, A. A., Pruitt, R. & Nürnberger, T. Sensing danger: key to activating plant immunity. *Trends Plant Sci.* **22**, 779–791 (2017).
13. Gully, K. et al. The SCOOP12 peptide regulates defense response and root elongation in *Arabidopsis thaliana*. *J. Exp. Bot.* **70**, 1349–1365 (2019).
14. Hou, S. et al. The *Arabidopsis* MIK2 receptor elicits immunity by sensing a conserved signature from phytocytokines and microbes. *Nat. Commun.* **12**, 5494 (2021).
15. Rhodes, J. et al. Perception of a divergent family of phytocytokines by the *Arabidopsis* receptor kinase MIK2. *Nat. Commun.* **12**, 705 (2021).

16. Guillou, M.-C. et al. The *PROSCOOP10* gene encodes two extracellular hydroxylated peptides and impacts flowering time in *Arabidopsis*. *Plants (Basel)* **11**, 3354 (2022).
17. Zhang, J. et al. EWR1 as a SCOOP peptide activates MIK2-dependent immunity in *Arabidopsis*.*J. Plant Inter.* **17**, 562–568 (2022).
18. Guillou, M. C. et al. SCOOP12 peptide acts on ROS homeostasis to modulate cell division and elongation in *Arabidopsis* primary root. *J. Exp. Bot.* **73**, 6115–6132 (2022).
19. Stahl, E. et al. The MIK2/SCOOP signaling system contributes to *Arabidopsis* resistance against herbivory by modulating jasmonate and indole glucosinolate biosynthesis. *Front. Plant Sci.* **13**, 852808 (2022).
20. Julkowska, M. M. et al. Natural variation in rosette size under salt stress conditions corresponds to developmental differences between *Arabidopsis* accessions and allelic variation in the *LRR-KISS* gene. *J. Exp. Bot.* **67**, 2127–2138 (2016).
21. Van der Does, D. et al. The *Arabidopsis* leucine-rich repeat receptor kinase MIK2/LRR-KISS connects cell wall integrity sensing, root growth and response to abiotic and biotic stresses. *PLoS Genet.* **13**, e1006832 (2017).
22. Engelsdorf, T. et al. The plant cell wall integrity maintenance and immune signaling systems cooperate to control stress responses in *Arabidopsis thaliana*. *Sci. Signal.* **11**, eaao3070 (2018).
23. Coleman, A. D. et al. The *Arabidopsis* leucine-rich repeat receptor-like kinase MIK2 is a crucial component of early immune responses to a fungal-derived elicitor. *New Phytol.* **229**, 3453–3466 (2021).
24. Stintzi, A. & Schaller, A. Biogenesis of post-translationally modified peptide signals for plant reproductive development. *Curr. Opin. Plant Biol.* **69**, 102274 (2022).
25. Royek, S. et al. Processing of a plant peptide hormone precursor facilitated by posttranslational tyrosine sulfation. *Proc. Natl Acad. Sci. USA* **119**, e2201195119 (2022).
26. Bailey, T. L. & Gribskov, M. Combining evidence using *p*-values: application to sequence homology searches. *Bioinformatics* **14**, 48–54 (1998).
27. Bjornson, M., Pimprikar, P., Nürnberger, T. & Zipfel, C. The transcriptional landscape of *Arabidopsis thaliana* pattern-triggered immunity. *Nat. Plants* **7**, 579–586 (2021).
28. Yu, Z. et al. The Brassicaceae-specific secreted peptides, STMPs, function in plant growth and pathogen defense. *J. Integr. Plant Biol.* **62**, 403–420 (2020).
29. Yadeta, K. A., Valkenburg, D. J., Hanemian, M., Marco, Y. & Thomma, B. P. The Brassicaceae-specific *EWR1* gene provides resistance to vascular wilt pathogens. *PLoS ONE* **9**, e88230 (2014).
30. Neukermans, J. et al. ARACINs, Brassicaceae-specific peptides exhibiting antifungal activities against necrotrophic pathogens in *Arabidopsis*. *Plant Physiol.* **167**, 1017–1029 (2015).
31. Petre, B. Toward the discovery of host-defense peptides in plants. *Front. Immun.* **11**, 1825 (2020).
32. Fletcher, J. C. Recent advances in *Arabidopsis* CLE peptide signaling. *Trends Plant Sci.* **25**, 1005–1016 (2020).
33. Liu, J. X., Srivastava, R., Che, P. & Howell, S. H. Salt stress responses in *Arabidopsis* utilize a signal transduction pathway related to endoplasmic reticulum stress signaling. *Plant J.* **51**, 897–909 (2007).
34. Liu, J. X., Srivastava, R., Che, P. & Howell, S. H. An endoplasmic reticulum stress response in *Arabidopsis* is mediated by proteolytic processing and nuclear relocation of a membrane-associated transcription factor, bZIP28. *Plant Cell* **19**, 4111–4119 (2007).
35. Ghorbani, S. et al. The SBT6.1 subtilase processes the GOLVEN1 peptide controlling cell elongation. *J. Exp. Bot.* **67**, 4877–4887 (2016).
36. Abarca, A., Franck, C. M. & Zipfel, C. Family-wide evaluation of RAPID ALKALINIZATION FACTOR peptides. *Plant Physiol.* **187**, 996–1010 (2021).
37. Sénéchal, F. et al. *Arabidopsis* PECTIN METHYLESTERASE17 is co-expressed with and processed by SBT3.5, a subtilisin-like serine protease. *Ann. Bot.* **114**, 1161–1175 (2014).
38. Hruz, T. et al. Genevestigator v3: a reference expression database for the meta-analysis of transcriptomes. *Adv. Bioinformatics* **2008**, 420747 (2008).
39. Schaller, A. et al. From structure to function – a family portrait of plant subtilases. *New Phytol.* **218**, 901–915 (2018).
40. Ramírez, V., López, A., Mauch-Mani, B., Gil, M. J. & Vera, P. An extracellular subtilase switch for immune priming in *Arabidopsis*. *PLoS Pathog.* **9**, e1003445 (2013).
41. Kourelis, J. et al. A homology-guided, genome-based proteome for improved proteomics in the alloploid *Nicotiana benthamiana*. *BMC Genomics* **20**, 722 (2019).
42. von Groll, U., Berger, D. & Altmann, T. The subtilisin-like serine protease SDD1 mediates cell-to-cell signaling during *Arabidopsis* stomatal development. *Plant Cell* **14**, 1527–1539 (2002).
43. Cedzich, A. et al. The protease-associated domain and C-terminal extension are required for zymogen processing, sorting within the secretory pathway, and activity of tomato subtilase 3 (SlSBT3). *J. Biol. Chem.* **284**, 14068–14078 (2009).
44. Ottmann, C. et al. Structural basis for Ca^{2+}-independence and activation by homodimerization of tomato subtilase 3. *Proc. Natl Acad. Sci. USA* **106**, 17223–17228 (2009).
45. Stührwohldt, N., Schardon, K., Stintzi, A. & Schaller, A. A toolbox for the analysis of peptide signal biogenesis. *Mol. Plant* **10**, 1023–1025 (2017).
46. Tian, M., Huitema, E., Da Cunha, L., Torto-Alalibo, T. & Kamoun, S. A Kazal-like extracellular serine protease inhibitor from *Phytophthora infestans* targets the tomato pathogenesis-related protease P69B. *J. Biol. Chem.* **279**, 26370–26377 (2004).
47. Tian, M., Benedetti, B. & Kamoun, S. A second Kazal-like protease inhibitor from *Phytophthora infestans* inhibits and interacts with the apoplastic pathogenesis-related protease P69B of tomato. *Plant Physiol.* **138**, 1785–1793 (2005).
48. Paulus, J. K. et al. Extracellular proteolytic cascade in tomato activates immune protease Rcr3. *Proc. Natl Acad. Sci. USA* **117**, 17409–17417 (2020).
49. Stührwohldt, N., Bühler, E., Sauter, M. & Schaller, A. Phytosulfokine (PSK) precursor processing by subtilase SBT3.8 and PSK signaling improve drought stress tolerance in *Arabidopsis*. *J. Exp. Bot.* **72**, 3427–3440 (2021).
50. Stegmann, M. et al. RGI-GOLVEN signaling promotes cell surface immune receptor abundance to regulate plant immunity. *EMBO Rep.* **23**, e53281 (2022).
51. Zhang, H. et al. A plant phytosulfokine peptide initiates auxin-dependent immunity through cytosolic Ca^{2+} signaling in tomato. *Plant Cell* **30**, 652–667 (2018).
52. Igarashi, D., Tsuda, K. & Katagiri, F. The peptide growth factor, phytosulfokine, attenuates pattern-triggered immunity. *Plant J.* **71**, 194–204 (2012).
53. Ranf, S. et al. Microbe-associated molecular pattern-induced calcium signaling requires the receptor-like cytoplasmic kinases, PBL1 and BIK1. *BMC Plant Biol.* **14**, 374 (2014).
54. Lampropoulos, A. et al. GreenGate—a novel, versatile, and efficient cloning system for plant transgenesis. *PLoS ONE* **8**, e83043 (2013).
55. Gleave, A. P. A versatile binary vector system with a T-DNA organisational structure conducive to efficient integration of cloned DNA into the plant genome. *Plant Mol. Biol.* **20**, 1203–1207 (1992).

56. Castel, B., Tomlinson, L., Locci, F., Yang, Y. & Jones, J. D. G. Optimization of T-DNA architecture for Cas9-mediated mutagenesis in *Arabidopsis*. *PLoS ONE* **14**, e0204778 (2019).
57. Frickey, T. & Lupas, A. CLANS: a Java application for visualizing protein families based on pairwise similarity. *Bioinformatics* **20**, 3702–3704 (2004).
58. Kesten, C. et al. Pathogen-induced pH changes regulate the growth-defense balance in plants. *EMBO J.* **38**, e101822 (2019).
59. Huerta, A. I., Kesten, C., Menna, A. L., Sancho-Andrés, G. & Sanchez-Rodriguez, C. In-plate quantitative characterization of *Arabidopsis thaliana* susceptibility to the fungal vascular pathogen fusarium oxysporum. *Curr. Protoc. Plant Biol.* **5**, e20113 (2020).

Acknowledgements

We thank past and present members of the Zipfel laboratory for helpful discussions and comments. B. Brandt and P. Köster are particularly thanked for their assistance with the cloning of the PROSCOOP cleavage constructs. P. Pimprikar is also thanked for her assistance with generation of the CRISPR mutants. We acknowledge generous funding to study plant immune signalling by the Gatsby Charitable Foundation (C.Z.), the Biotechnology and Biological Research Council (BB/P012574/1) (C.Z.), the European Research Council under the European Union's Horizon 2020 research and innovation programme no. 773153 (project 'IMMUNO-PEPTALK') (C.Z.) and programme no. 724321 (project 'Sense2SurviveSalt') (C.T.), the University of Zurich (C.Z.) and the Swiss National Science Foundation grants no. 31003A_182625 (C.Z.) and 310030_184769 (C.S.R.).

Author contributions

H.Y., J.R. and C.Z. conceived and designed the experiments. H.Y., J.R., X.K., J.S., S.A., G.S.A., E.S., M.-C.G., N.G.-B, L.T.V.C. and K.W.B. generated materials, performed experiments and/or analysed the data. P.R., C.S.R., A. Stintzi, C.T., J.P.R., F.L.H.M., A. Schaller, J.R. and C.Z. supervised the project. H.Y., J.R. and C.Z. wrote the manuscript with input from all authors.

Competing interests

The authors declare no competing interests.

Additional information

Extended data is available for this paper at https://doi.org/10.1038/s41477-023-01583-x.

Supplementary information The online version contains supplementary material available at https://doi.org/10.1038/s41477-023-01583-x.

Correspondence and requests for materials should be addressed to Jack Rhodes or Cyril Zipfel.

Peer review information *Nature Plants* thanks Herman Hofte and the other, anonymous, reviewer(s) for their contribution to the peer review of this work.

Reprints and permissions information is available at www.nature.com/reprints.

Publisher's note Springer Nature remains neutral with regard to jurisdictional claims in published maps and institutional affiliations.

[1]Institute of Plant and Microbial Biology, Zurich-Basel Plant Science Center, University of Zurich, Zurich, Switzerland. [2]The Sainsbury Laboratory, University of East Anglia, Norwich Research Park, Norwich, UK. [3]Université Angers, Institut Agro, INRAE, IRHS, SFR QUASAV, Angers, France. [4]Institute of Molecular Plant Biology, ETH Zurich, Zurich, Switzerland. [5]Department of Plant Molecular Biology, University of Lausanne, Lausanne, Switzerland. [6]Laboratory of Plant Physiology, Wageningen University and Research, Wageningen, the Netherlands. [7]Institute of Biology, Plant Physiology and Biochemistry, University of Hohenheim, Stuttgart, Germany. [8]Present address: Institute of Genetics and Developmental Biology, Chinese Academy of Sciences, Beijing, China. [9]Present address: Plant Stress Resilience, Institute of Environmental Biology, Utrecht University, Utrecht, the Netherlands. ✉e-mail: jack.rhodes@tsl.ac.uk; cyril.zipfel@botinst.uzh.ch

https://doi.org/10.1038/s41477-023-01583-x

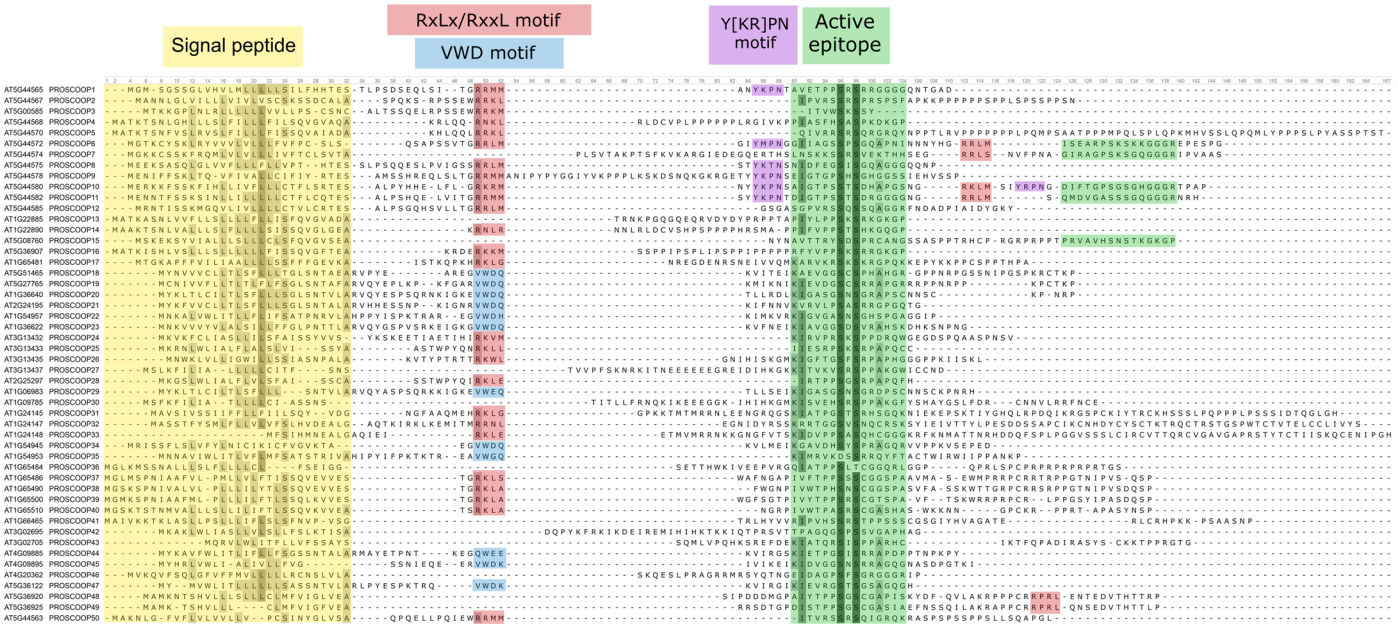

Extended Data Fig. 1 | Sequence alignment of *Arabidopsis* PROSCOOPs. Signal peptide, variable regions containing the predicted cleavage motifs RxLx/RxxL/VWD, and the active epitope containing the conserved motif SxS are indicated by coloured boxes.

https://doi.org/10.1038/s41477-023-01583-x

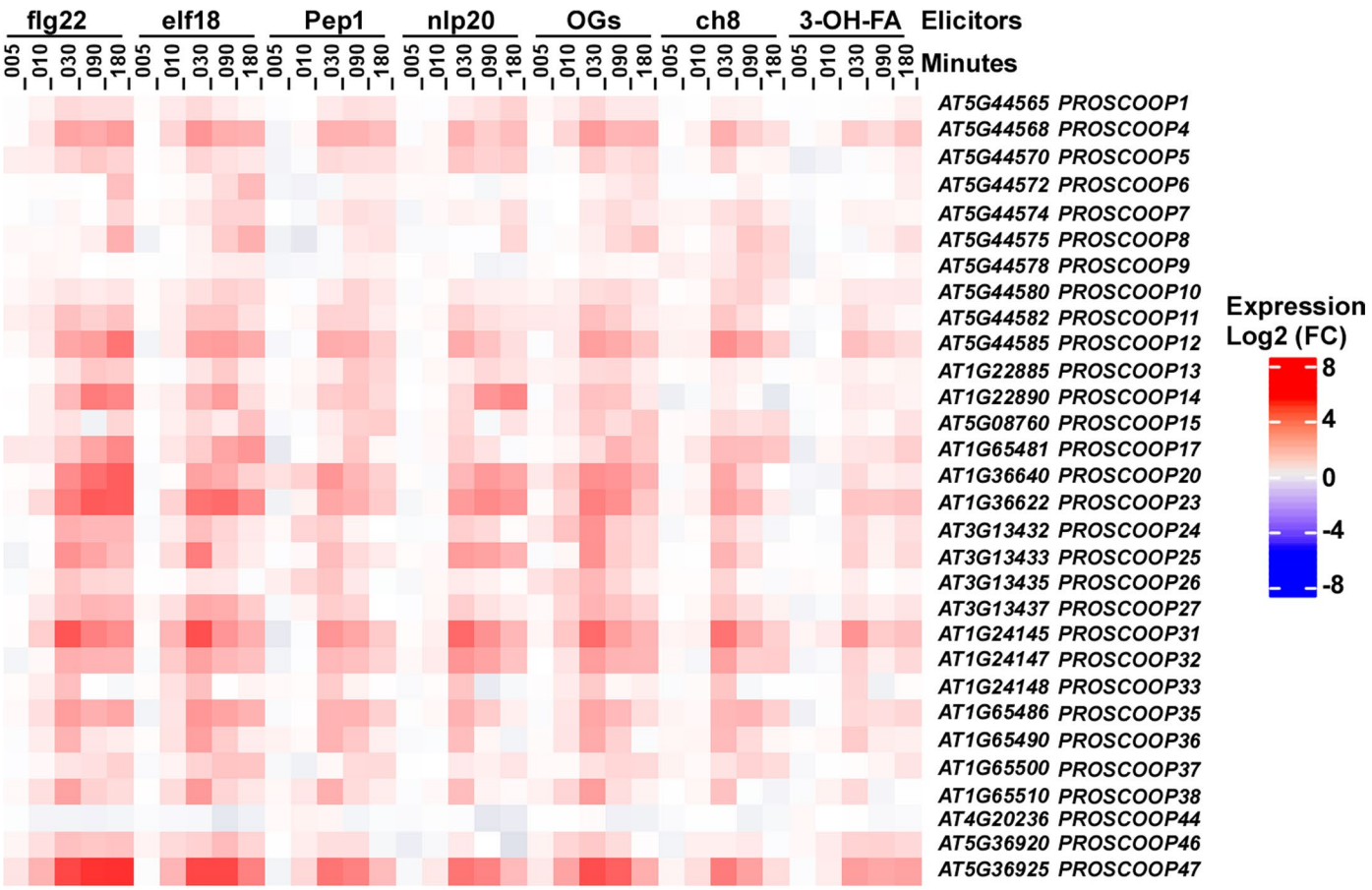

Extended Data Fig. 2 | All *PROSCOOP*s identified by RNA-Seq are up-regulated upon elicitor treatment. Heat map showing $\log_2$(FC) expression levels of *PROSCOOP*s identified by RNA-Seq in response to a range of elicitors (data obtained from[27]).

https://doi.org/10.1038/s41477-023-01583-x

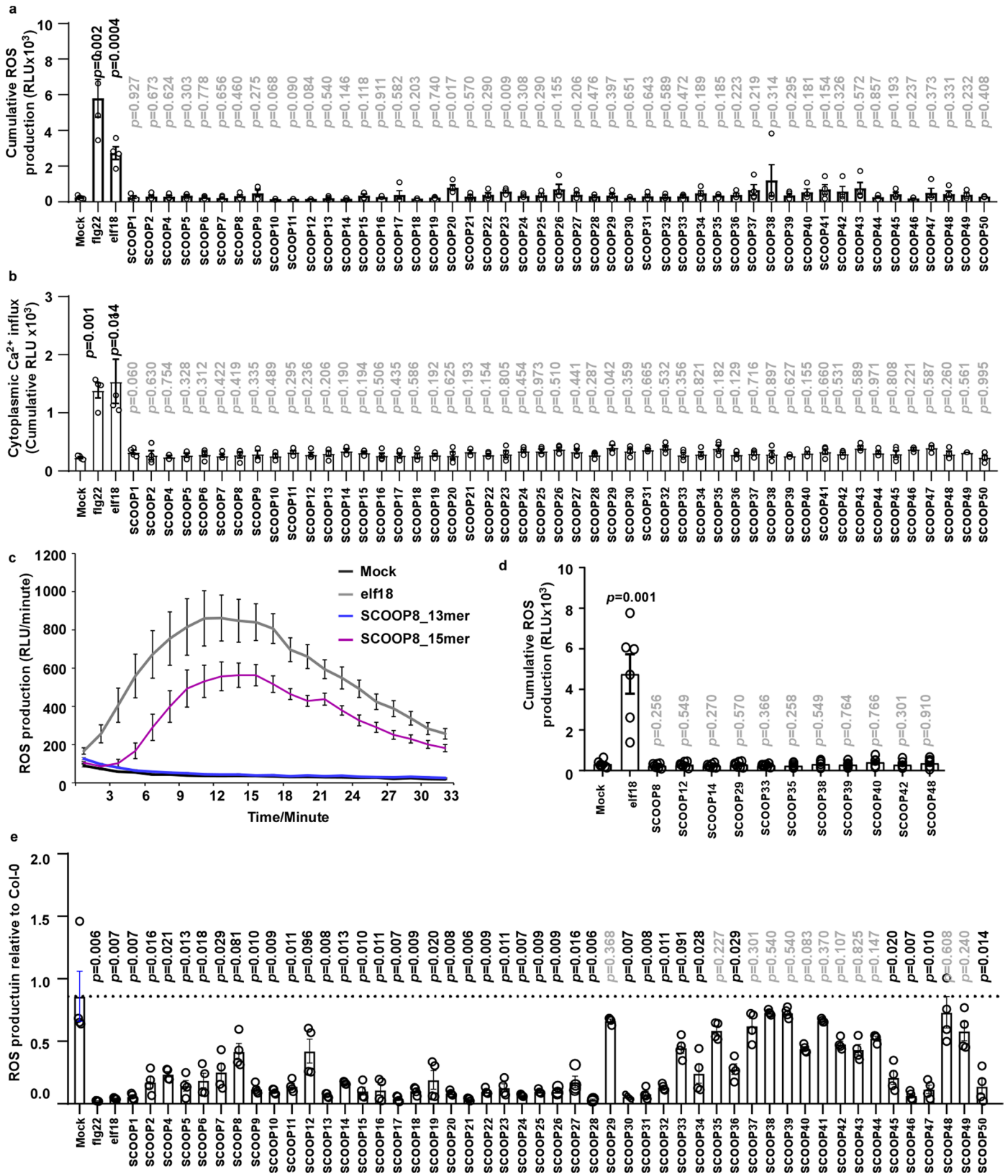

Extended Data Fig. 3 | See next page for caption.

https://doi.org/10.1038/s41477-023-01583-x

Extended Data Fig. 3 | Divergent SCOOPs-induced responses. (**a**) Integrated ROS production over 40 min in leaf disks collected from 4-week-old *Arabidopsis mik2-1* plants induced in the absence (Mock) or presence of 1 µM 13-mer SCOOPs peptides (n = 4) using 100 nM flg22 and elf18 as control. (**b**) Cytoplasmic Ca^{2+} influx measured in *mik2-1*^{AEQ} seedlings induced in the absence (Mock) or presence of 1 µM 13-mer SCOOPs peptides (n = 4) using 100 nM flg22 and elf18 as control. (**c**) Integrated ROS production over 40 min in leaf disks collected from 4-week-old *Arabidopsis* plants induced in the absence (Mock) or presence of 1 µM 13/15-mer SCOOP8 peptides (n = 8) using 100 nM elf18 as control. (**d**) Integrated ROS production over 40 min in leaf disks collected from 4-week-old *Arabidopsis mik2-1* plants induced in the absence (Mock) or presence of 15-mer SCOOPs (n = 6) using 100 nM elf18 as control. (**e**) Integrated ROS production over 40 min in leaf disks collected from 4-week-old *Arabidopsis bak1-5 bkk1* plants relative to Col-0 induced in the absence (Mock) or presence of 1 µM 13-mer SCOOPs peptides (n = 4) using 100 nM flg22 and elf18 as control. (a-e) Data represents the mean ± SD; P-values indicate significance relative to the Mock in a Two-tailed T-test. All experiments were repeated and analysed three times with similar results.

https://doi.org/10.1038/s41477-023-01583-x

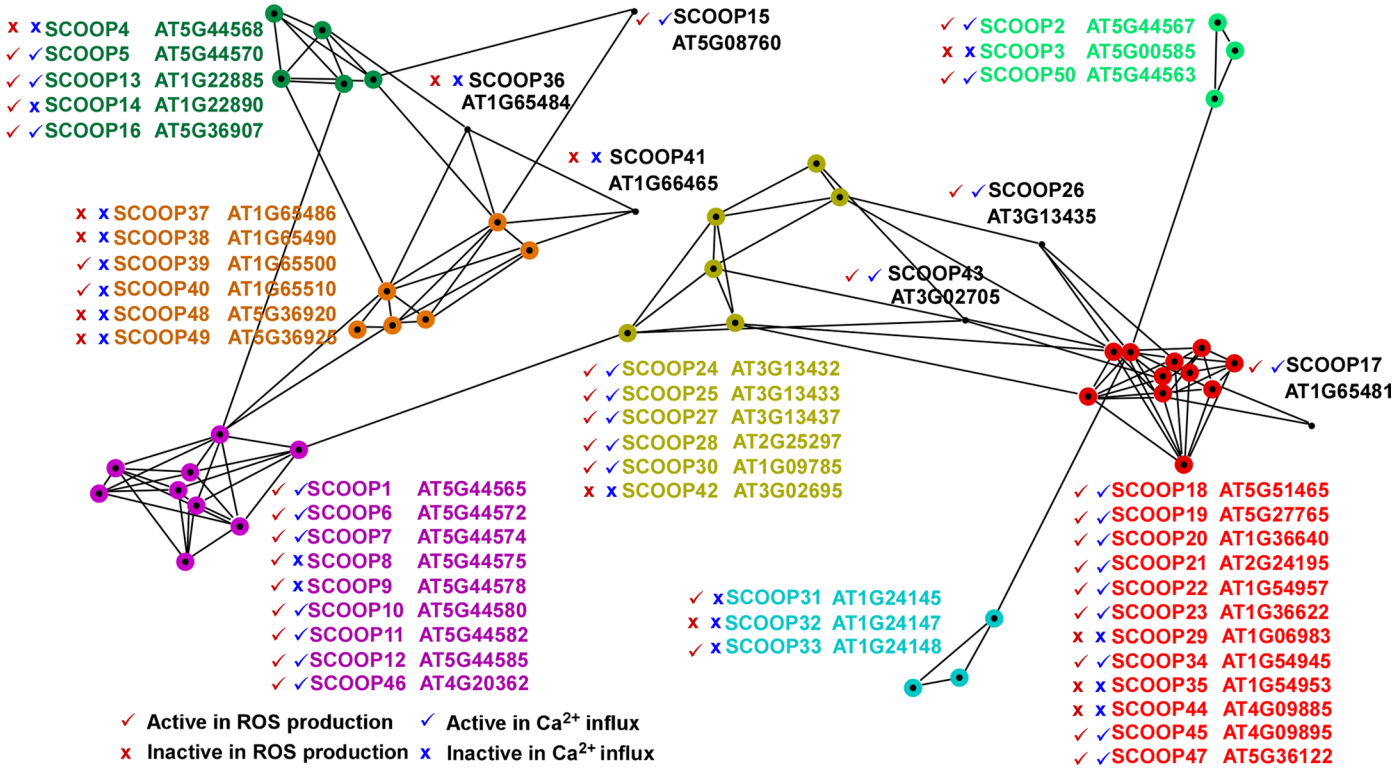

Extended Data Fig. 4 | Similarity relationships inside the PROSCOOP family and summary of SCOOPs activity in Col-0. CLANS clustering based on all-against-all pairwise sequence similarities resulted in 7 groups (highlighted with different colours) and 6 singletons. P-values lower than 1.E-2 and 1.E-5 are represented by grey and black edges respectively. Coloured asterisk indicates effects of SCOOP peptides.

https://doi.org/10.1038/s41477-023-01583-x

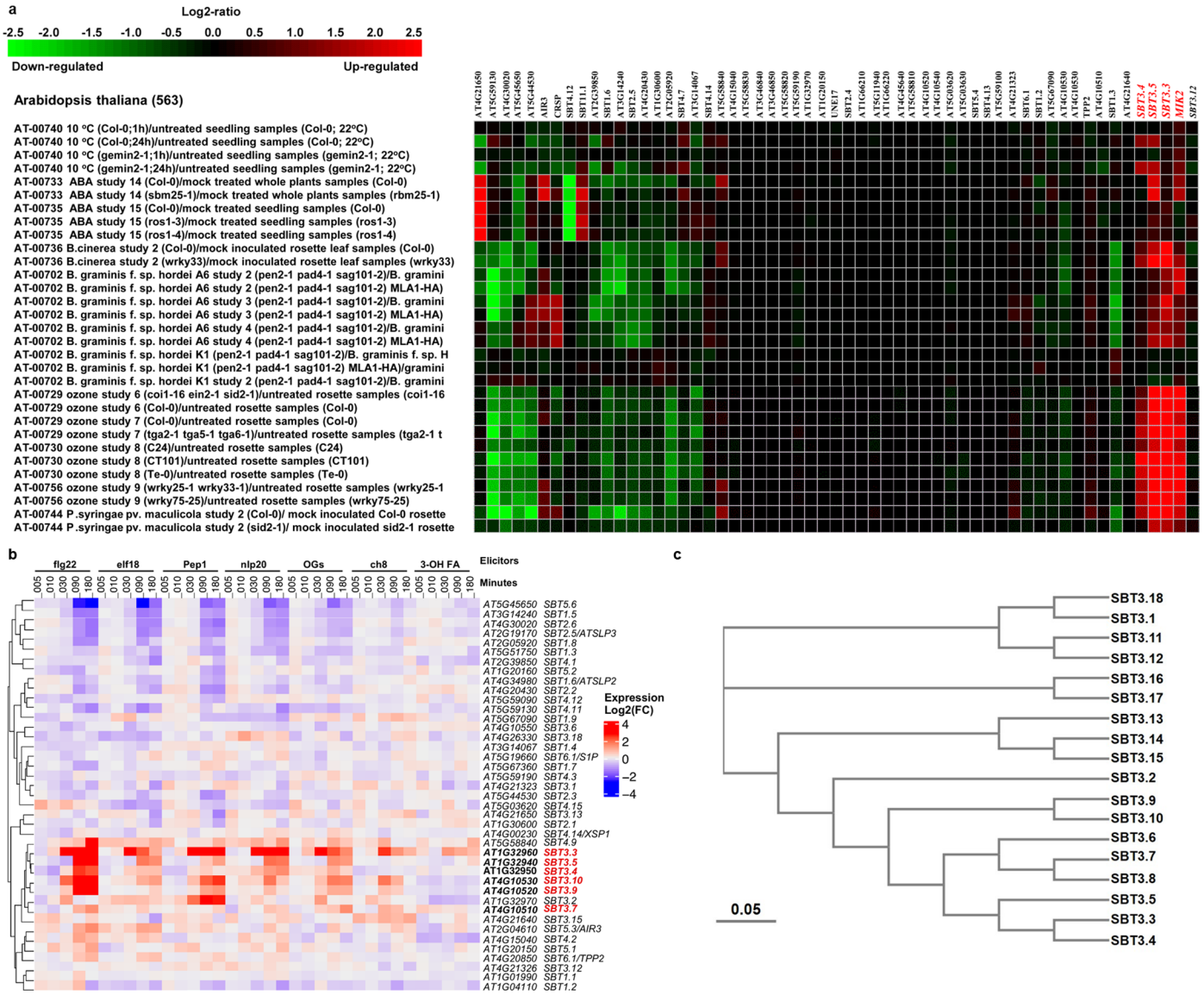

Extended Data Fig. 5 | Analysis of *SBT3* subgroup. (**a**) SBT3.3/3.4/3.5 are co-regulated with MIK2 in response to different stresses. Heat map showing log2(FC) expression levels of SBTs in response to stresses (data obtained from Genevestigator). (**b**) Transcriptional regulation of Arabidopsis SBT genes by elicitors. Heat map showing log2(FC) expression levels of SBT genes in response to a range of elicitors (data obtained from[27]). (**c**) Phylogeny of Arabidopsis SBT3 subgroup. Phylogeny of the full-length amino acid sequences of SBT3 was inferred using the online T-coffee server (https://tcoffee.crg.eu/apps/tcoffee/do:mcoffee).

https://doi.org/10.1038/s41477-023-01583-x

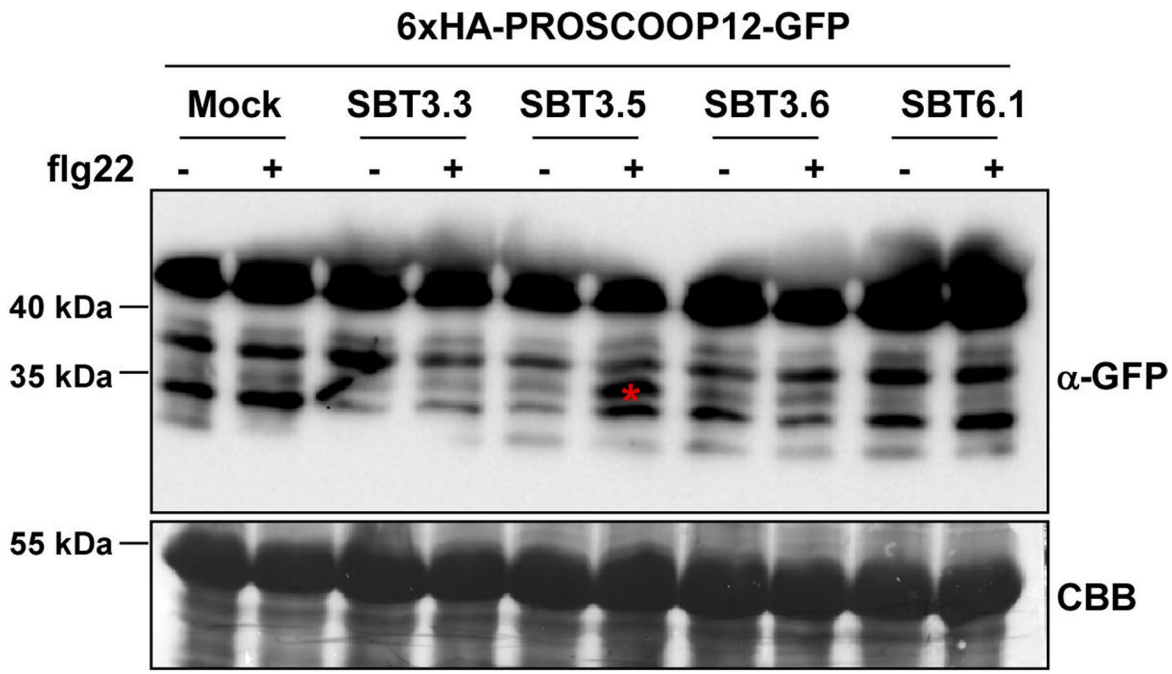

Extended Data Fig. 6 | Cleavage analysis of PROSCOOP12 and PROSCOOP20 by different SBTs. Related to Fig. 2b, indicating flg22-induced SBT3.5-mediated PROSCOOP12 cleavage.

https://doi.org/10.1038/s41477-023-01583-x

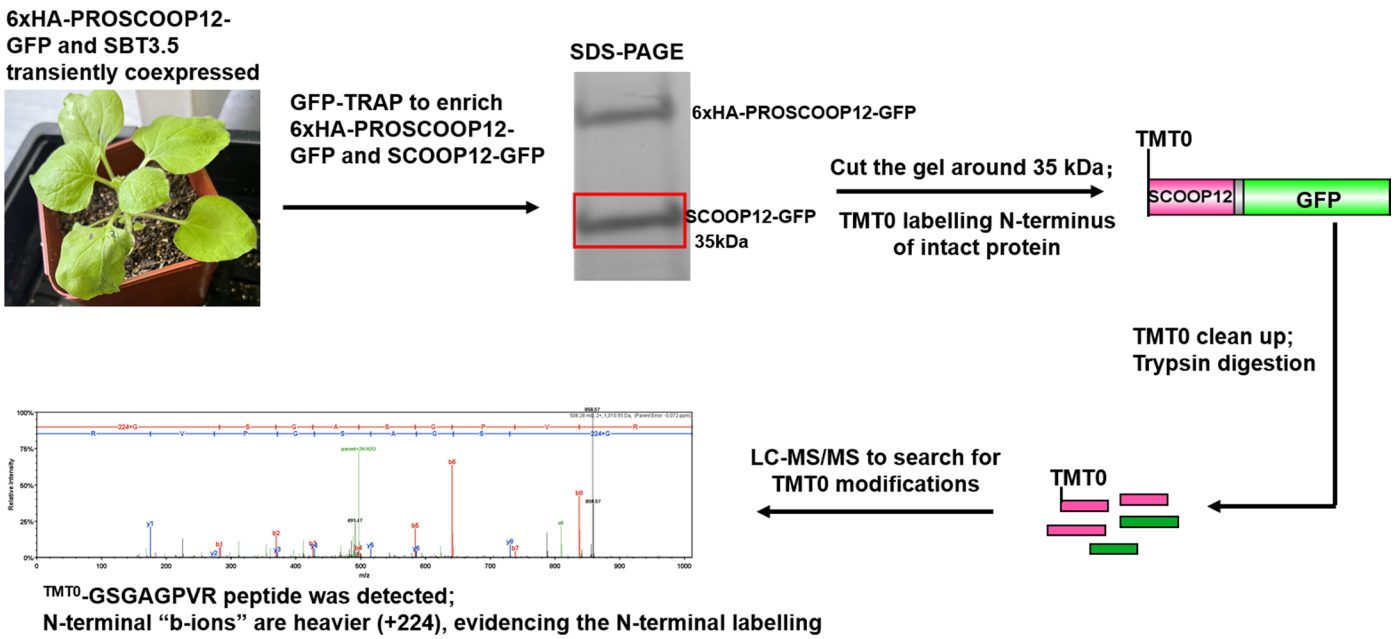

Extended Data Fig. 7 | The diagram of TMT-labelling coupled MS. The working flow of TMT-labelling coupled MS to identify SBT3.5-mediated 6xHA-PROSCOOP12-GFP cleavage sites and SBT3.6-mediated 6xHA-PROSCOOP20-GFP cleavage sites in *Nicotiana benthamiana*.

https://doi.org/10.1038/s41477-023-01583-x

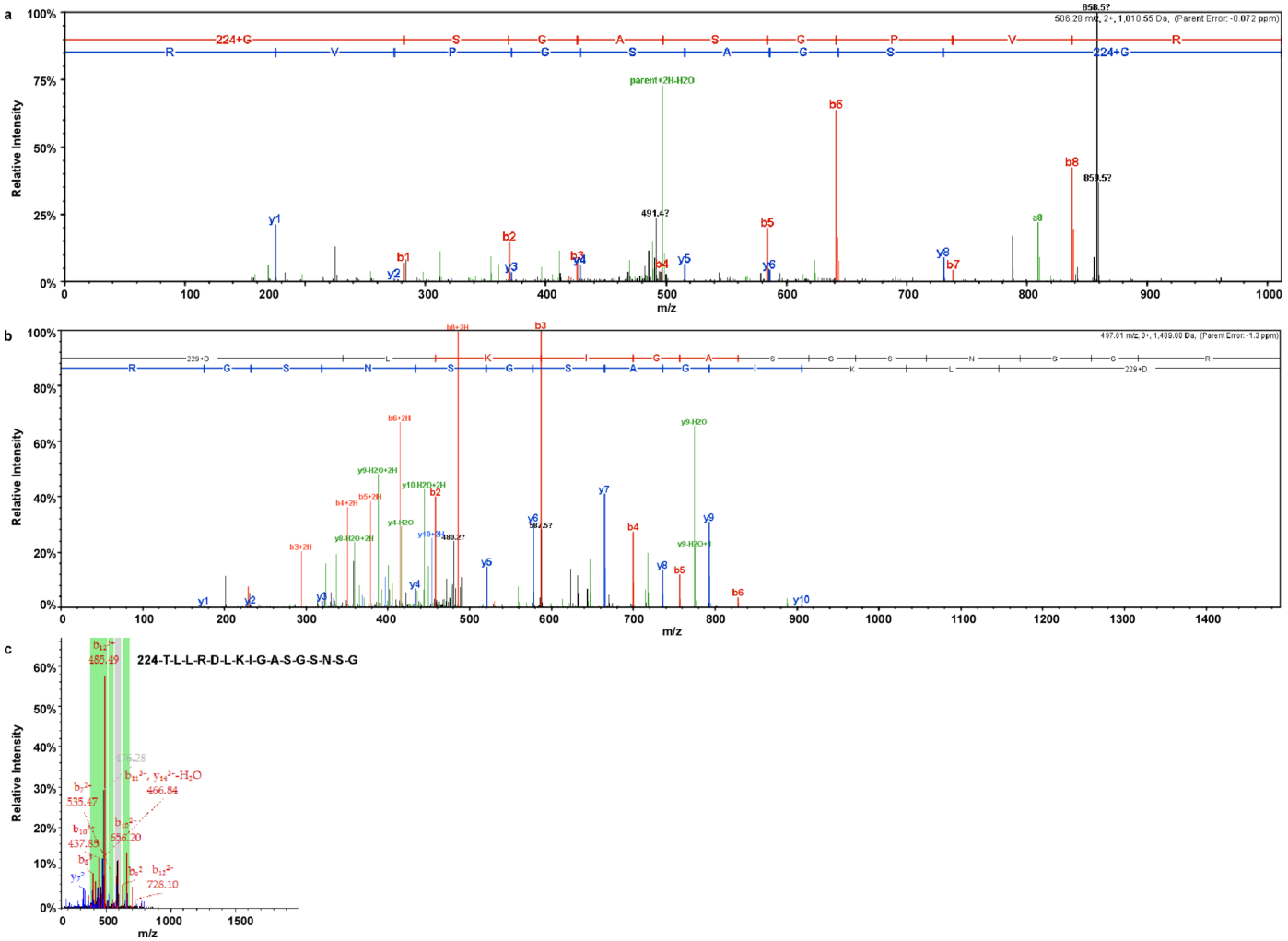

Extended Data Fig. 8 | Mass spectrometry of TMT labelling peptide. (**a**) TMT-GSGAGPVR peptide was detected by N-terminal labelling-coupled mass spectrometry with three independent experiments. (**b**) TMT-DLKIGASGSNSG peptide was detected by N-terminal labelling-coupled mass spectrometry with three independent experiments. (**c**) TMT-TLLRDLKIGASGSNSG peptide was detected by N-terminal labelling-coupled mass spectrometry with only one time from three repeats.

https://doi.org/10.1038/s41477-023-01583-x

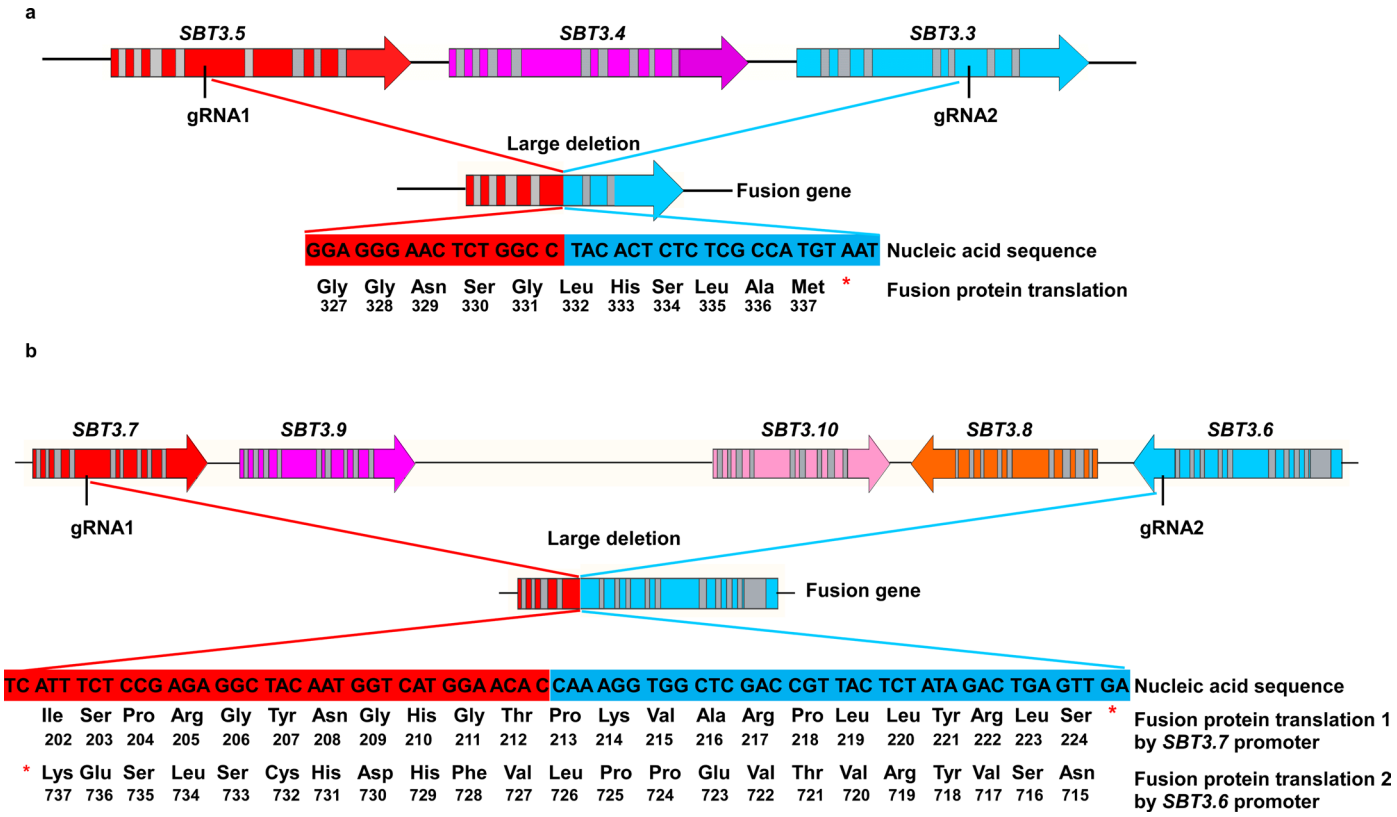

Extended Data Fig. 9 | CRISPR deletes the majority of *SBT3.3/3.4/3.5* and *SBT3.6/3.7/3.8/3.9/3.10* genomic region. (**a**) Schematic view of the large genomic deletion of clusters *SBT3.3/3.4/3.5*. The fusion protein may be transcribed, consisting of the first 331 amino acids of SBT3.5 with an out-of-frame fusion with SBT3.3 leading to an early stop. Primers F1/R1 and F2/R2 used for the genotyping and sequence (Supplementary Table 3). (**b**) Schematic view of the large genomic deletion of clusters *SBT3.6/3.7/3.8/3.9/3.10*. One fusion protein driven by the promoter *SBT3.7* may be transcribed, consisting of 212 amino acid of SBT3.7, fused to 12 nonsense amino acids from SBT3.6 genomic region. Another fusion protein driven by the promoter *SBT3.6* may be transcribed, consisting of 726 amino acids of SBT3.6, fused to 11 nonsense amino acids from SBT3.7 genomic region. Primers F3/R3 and F4/R4 used for the genotyping and sequence (Supplementary Table 3).

https://doi.org/10.1038/s41477-023-01583-x

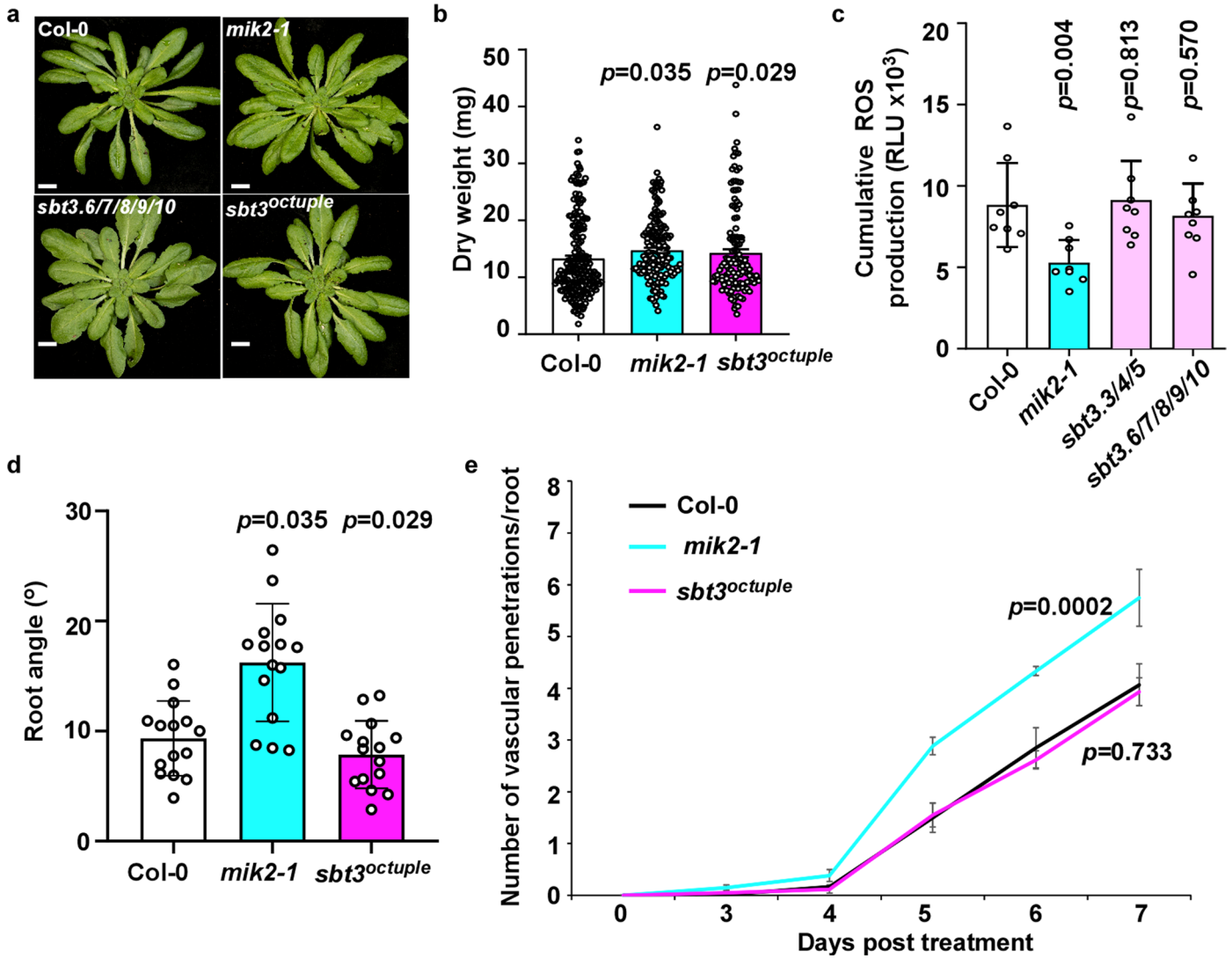

Extended Data Fig. 10 | Phenotypic analysis of *sbt* higher-order mutants. (**a**) Phenotype of 5-week-old plants. Bar = 1cm. (**b**) Dry weight of 4-week-old plants. One week after germination, plants were transferred to pots with soil watered from below in demineralized water. After 3 weeks the rosettes were cut, and dry weight was determined. Data represents the mean ± SD of three independent experiments. P-values indicate significance relative to Col-0 in a two-sided T-test. Number of individual larvae measured: Col-0 n = 191, *mik2-1* n = 160 and *sbt3*^{octuple} n = 143. (**c**) Integrated ROS production over 30 min in leaf disks collected from 4-week-old Arabidopsis plants induced by 100 nM flg22 application (n = 8). (**d**) Quantification of the root angle of 9-day-old seedlings grown in an upright position on MS agar medium (n = 15). (**e**) Cumulative Arabidopsis root vascular penetration by Fo5176 in WT (Col-0), *mik2-1*, and *sbt3*^{octuple} plants at different days post transfer (dpt) to plate-containing spores (n = 60). Data represents the mean ± SD of three independent experiments. Statistical significance calculated via repeated measures two-way ANOVA with Tukey post-hoc test (p value ≤ 0.05 (genotype), p value ≤ 0.05 (time). P values are indicated in the graph with respect to WT at any dpt. (b-d) Data represents the mean ± SD; P-values indicate significance relative to Col-0 in a Two-tailed T-test. All experiments were repeated and analysed three times with similar results.

nature portfolio

Corresponding author(s): Cyril Zipfel
Jack Rhodes

Last updated by author(s): Oct 16, 2023

Reporting Summary

Nature Portfolio wishes to improve the reproducibility of the work that we publish. This form provides structure for consistency and transparency in reporting. For further information on Nature Portfolio policies, see our Editorial Policies and the Editorial Policy Checklist.

Statistics

For all statistical analyses, confirm that the following items are present in the figure legend, table legend, main text, or Methods section.

n/a	Confirmed	
☐	☒	The exact sample size (*n*) for each experimental group/condition, given as a discrete number and unit of measurement
☐	☒	A statement on whether measurements were taken from distinct samples or whether the same sample was measured repeatedly
☐	☒	The statistical test(s) used AND whether they are one- or two-sided *Only common tests should be described solely by name; describe more complex techniques in the Methods section.*
☒	☐	A description of all covariates tested
☐	☒	A description of any assumptions or corrections, such as tests of normality and adjustment for multiple comparisons
☐	☒	A full description of the statistical parameters including central tendency (e.g. means) or other basic estimates (e.g. regression coefficient) AND variation (e.g. standard deviation) or associated estimates of uncertainty (e.g. confidence intervals)
☐	☒	For null hypothesis testing, the test statistic (e.g. *F*, *t*, *r*) with confidence intervals, effect sizes, degrees of freedom and *P* value noted *Give P values as exact values whenever suitable.*
☒	☐	For Bayesian analysis, information on the choice of priors and Markov chain Monte Carlo settings
☒	☐	For hierarchical and complex designs, identification of the appropriate level for tests and full reporting of outcomes
☒	☐	Estimates of effect sizes (e.g. Cohen's *d*, Pearson's *r*), indicating how they were calculated

Our web collection on statistics for biologists contains articles on many of the points above.

Software and code

Policy information about availability of computer code

Data collection	Genevestigator software used to collect the expression levels of SBTs in response to stresses (https://genevestigator.com/) ROS data: Image32 (Photek, St Leonards on Sea, UK) Calcium data: SkanIt™ (Thermo Fisher Scientific) MAST (part of the MEME suite; doi.org/10.1093/bioinformatics/14.1.48) the online T-coffee server (https://tcoffee.crg.eu/apps/tcoffee/do:mcoffee) used to analysis SBT3 subgroup Phylogeny
Data analysis	ImageJ V1.8.0 software used to analyze root length (https://imagej.net/software/fiji/) CLANS software to analyze PROSCOOP clustering (doi.org/10.1016/j.jmb.2017.12.007) Statistical analysis: GraphPad Prism v.10

For manuscripts utilizing custom algorithms or software that are central to the research but not yet described in published literature, software must be made available to editors and reviewers. We strongly encourage code deposition in a community repository (e.g. GitHub). See the Nature Portfolio guidelines for submitting code & software for further information.

Data

Policy information about availability of data

All manuscripts must include a data availability statement. This statement should provide the following information, where applicable:

- Accession codes, unique identifiers, or web links for publicly available datasets
- A description of any restrictions on data availability
- For clinical datasets or third party data, please ensure that the statement adheres to our policy

The authors declare that the data supporting the findings of this study are available within the manuscript and its supplementary files. Raw data for underlying Figs. 1a-c, 4a-e and Extended Data Figs 3a-e, 10b-e are provided in the Source Data file.
The Arabidopsis Col-0 genome (with Araport11 annotation) was used to identify PROSCOOP sequences (https://www.arabidopsis.org/download/index-auto.jsp?dir=%2Fdownload_files%2FGenes%2FAraport11_genome_release)

Human research participants

Policy information about studies involving human research participants and Sex and Gender in Research.

Reporting on sex and gender	N/A
Population characteristics	N/A
Recruitment	N/A
Ethics oversight	N/A

Note that full information on the approval of the study protocol must also be provided in the manuscript.

Field-specific reporting

Please select the one below that is the best fit for your research. If you are not sure, read the appropriate sections before making your selection.

☒ Life sciences ☐ Behavioural & social sciences ☐ Ecological, evolutionary & environmental sciences

For a reference copy of the document with all sections, see nature.com/documents/nr-reporting-summary-flat.pdf

Life sciences study design

All studies must disclose on these points even when the disclosure is negative.

Sample size	No sample size calculation was performed. Sample size was chosen as large as possible (e.g. given limitations on plate size) and in accordance with previous established protocols in the field. Given the sample size, adequate statistical analysis was performed.
Data exclusions	No data were excluded
Replication	All findings were successfully reproduced in several (atleast 3) replicates as described in figure legends and methods.
Randomization	Sampling of leaf discs was performed by randomly selecting uniform leaves from individual plants grown in standard conditions and with different genotypes grown in the same growth chamber. For rosette images plants were grown in the same tray under standard conditions at the same time. Randomization was not relevant to biochemical assays in this study due to discrete controls.
Blinding	Blinding was not relevant for the biochemical assays in this experiment due to discrete controls. For other assays data collection was automated or bias could not affect data collection.

Reporting for specific materials, systems and methods

We require information from authors about some types of materials, experimental systems and methods used in many studies. Here, indicate whether each material, system or method listed is relevant to your study. If you are not sure if a list item applies to your research, read the appropriate section before selecting a response.

Materials & experimental systems

n/a	Involved in the study
☐	☒ Antibodies
☒	☐ Eukaryotic cell lines
☒	☐ Palaeontology and archaeology
☐	☒ Animals and other organisms
☒	☐ Clinical data
☒	☐ Dual use research of concern

Methods

n/a	Involved in the study
☒	☐ ChIP-seq
☒	☐ Flow cytometry
☒	☐ MRI-based neuroimaging

Antibodies

Antibodies used	α-HA-HRP (Roche 12013819001, 1:3000 dilution, lot #14847700) and α-GFP-HRP (Santa Cruz sc-9996, 1:5000 dilution, lot #L0419)
Validation	Validation statements for commercial antibodies are available from the corresponding manufacturers' websites.

Animals and other research organisms

Policy information about studies involving animals; ARRIVE guidelines recommended for reporting animal research, and Sex and Gender in Research

Laboratory animals	This study did not involve laboratory animals
Wild animals	The study did not involve wild animals.
Reporting on sex	N/A
Field-collected samples	The study did not involve samples collected from field.
Ethics oversight	The study did not require an Ethics approval.

Note that full information on the approval of the study protocol must also be provided in the manuscript.